RIGA TECHNICAL UNIVERSITY

Aleksandrs Korņejevs

RESEARCH AND DEVELOPMENT OF SELF-LEARNING NEURAL NETWORK ALGORITHM FOR OPTIMAL ENERGY-EFFICIENT AUTONOMOUS ELECTRICAL UNMANNED VEHICLES MOTION CONTROL

Summary of the Doctoral Thesis

RTU Press
Riga 2023

RIGA TECHNICAL UNIVERSITY
Faculty of Electrical and Environmental Engineering
Institute of Industrial Electronics and Electrical Engineering

Aleksandrs Korņejevs
Doctoral Student of the Study Programme "Computer Control of Electrical Technology"

RESEARCH AND DEVELOPMENT OF SELF-LEARNING NEURAL NETWORK ALGORITHM FOR OPTIMAL ENERGY-EFFICIENT AUTONOMOUS UNMANNED ELECTRICAL VEHICLES MOTION CONTROL

Summary of the Doctoral Thesis

Scientific supervisor
Professor Dr. sc. ing.
MIHAILS GOROBECS

RTU Press
Riga 2023

Korņejevs, A. Research and Development of Self-learning Neural Network Algorithm for Optimal Energy-efficient Autonomous Electrical Unmanned Vehicles Motion Control. Summary of the Doctoral Thesis. Riga: RTU Press, 2023. 40 p.

Published in accordance with the decision of the Promotion Council "P-14" of 4 October 2023, Minutes No. 04030-9.12.2/5.

This work was supported by the European Social Fund within Project No. 8.2.2.0/20/I/008, "Strengthening of PhD students and academic personnel of Riga Technical University and BA School of Business and Finance in the strategic fields of specialization" of the Specific Objective 8.2.2 "To Strengthen Academic Staff of Higher Education Institutions in Strategic Specialization Areas" of the Operational Programme "Growth and Employment".

Cover picture by Aleksandrs Korņejevs using *DALL-E*.

https://doi.org/10.7250/9789934370182
ISBN 978-9934-37-018-2 (pdf)

DOCTORAL THESIS PROPOSED TO RIGA TECHNICAL UNIVERSITY FOR THE PROMOTION TO THE SCIENTIFIC DEGREE OF DOCTOR OF SCIENCE

To be granted the scientific degree of Doctor of Science (Ph. D.), the present Doctoral Thesis has been submitted for defence at the open meeting of RTU Promotion Council on 29 December 2023 at 9.30 at the Faculty of Electrical and Environmental Engineering of Riga Technical University, 12/1 Āzenes Street, Room 212.

OFFICIAL REVIEWERS

Professor Dr. sc. ing. Nadežda Kuņicina
Riga Technical University

Researcher Dr. sc. ing. Artjoms Obuševs
Zurich University of Applied Science, Switzerland

Associate Professor Ph. D. Augusto Montisci
Università degli Studi di Cagliari, Italy

DECLARATION OF ACADEMIC INTEGRITY

I hereby declare that the Doctoral Thesis submitted for review to Riga Technical University for promotion to the scientific degree of Doctor of Science (Ph. D.) is my own. I confirm that this Doctoral Thesis has not been submitted to any other university for promotion to a scientific degree.

Name Surname ……. (signature)
Date: ……

The Doctoral Thesis has been written in English. It consists of an Introduction, 4 chapters, Conclusions, 84 figures, and 8 tables; the total number of pages is 126. The Bibliography contains 92 titles.

Table of contents

Relevance of the topic

The Thesis aims to research and develop an adaptive control system algorithm, its implementation, and integration into the control system of an existing unmanned vehicle. An additional optimization controller is proposed for energy-efficient control of unmanned vehicle movement. The structure based on a neural network expands the adaptive search algorithm, significantly reducing the time required to determine the optimal control signal values and maximizing the energy efficiency of the unmanned vehicle. The proposed approach is intended to be universally applicable to any unmanned vehicle with varying numbers of propulsion systems, different or variable masses, and other configuration differences, without any initial manual tuning. Any electric unmanned vehicle should move with maximum energy efficiency using the suggested algorithm.

Scientific publications on this subject have been analyzed to gain insights into the current state of research, innovative technologies, and potential solutions (the most relevant are referenced at the end of the Thesis). The study aims to understand the existing knowledge, identify emerging trends, and explore opportunities for further improvements in optimizing electric transportation systems, including the integration of autonomous features. Analysis reveals that currently, the majority of energy-saving solutions are related to route calculation and trajectory planning for unmanned vehicles (UVs), as well as energy-saving algorithms for other equipment unrelated to UV electric propulsion systems. Only a few studies focused on reducing energy consumption explore the mechanical and electrical properties of power devices.

The goal and tasks of the thesis

The goal of the research

The goal of the research is to develop a method for optimizing the power consumption of any electric unmanned vehicle. This method will enable determining optimal control signals at the beginning of motion for efficient energy control under varying vehicle parameters, without prior calculations or adjustments.

Hypothesis

Using the new method can reduce the energy consumption of unmanned vehicles.

The tasks of the research

- Research the mechanical and electrical properties of electric motors for unmanned electric vehicles.
- Develop a mathematical model of unmanned electric vehicles to solve the energy consumption minimization problem.
- Construct mechanical models of electric unmanned vehicles.
- Identify the target function for minimizing energy consumption.
- Explore algorithms for finding minimal energy consumption.
- Research neural networks.
- Research and develop an algorithm for automatic creation of a training set.
- Develop an optimization algorithm for a self-learning neural network.
- Design an electrical circuit for the optimization controller.
- Develop electrical circuits for experimental devices.
- Create a computer model of unmanned electric vehicles for experimental energy consumption calculations and investigation of the optimized objective function.
- Experimentally test various traction electric motors for unmanned electric vehicles and collect data on their performance and consumption.

- Test the optimization algorithm of the self-learning neural network.

Research tools and methods

- Inductive method
- Deductive method
- Systems analysis
- Statistical analysis methods
- Neural network theory
- Optimization methods
- Formalization method

Scientific novelty of the work

A new method for energy savings in electric unmanned vehicles has been developed. The method consists of a new algorithm for automatic generation of a training dataset for a neural network, a new algorithm for load characterization, and a minimum search algorithm.

The novelty of the proposed method is in the self-learning neural network and the algorithm for this network to determine the nature of the load and its change.

Practical application of the work

The application of this method enhances energy efficiency and reduces power consumption in electric unmanned vehicles. The developed optimization controller can be utilized in any electric unmanned vehicle.

Work approbation

1. 61st International Scientific Conference on Power and Electrical Engineering of Riga Technical University, report "Neural Network-Based UAV Optimal Control Algorithm for Energy Efficiency Maximization", A. Korneyev, M. Gorobetz, Latvia, Riga, 5–7 November 2020.
2. 59th International Scientific Conference on Power and Electrical Engineering of Riga Technical University, report "Unified Energy Efficient Control Algorithm for Electric Unmanned Aerial Vehicles with Different Traction Drives and Configurations," A. Korneyev, M. Gorobetz, A. Levchenkov, Latvia, Riga, 12–14 November 2018.
3. 60th International Scientific Conference on Power and Electrical Engineering of Riga Technical University, report "Analysis and Modelling of UAV Electrical Traction Drive based on Empirical Data for Energy Efficiency Tasks," M. Gorobetz, A. Potapovs, A. Korneyev, Latvia, Riga, 7–9 October, 2019.
4. 7th IEEE International Energy Conference, report referāts "Long-term Energy and Fuel Consumption Forecast in Private and Commercial Transport using Artificial Life Approach," M. Gorobetz, A. Korneyev, L. Zemite, Latvia, Riga, 9–12 May 2022.
5. 61st International Scientific Conference on Power and Electrical Engineering of Riga Technical University, report "Intelligent Algorithm for Using Overall Energy Consumption Statistics," M. Gorobetz, L. Zemite, A. Jasevics, A. Korneyev, Latvia, Riga, 5–7 November 2020.
6. 11th International Doctoral School of Energy Conversion and Saving Technologies, report "Research and development of evolutionary algorithms for optimal energy efficient control of autonomous unmanned electric vehicle systems," Latvia, Klapkalnciems, 27–28 May 2022

Author's publications

1. **A. Korneyev**, M. Gorobetz. Neural Network Based UAV Optimal Control Algorithm for Energy Efficiency Maximization, 2020 IEEE 61st International Scientific Conference on Power and Electrical Engineering of Riga Technical University (RTUCON 2020), Latvia, Riga, 5–7 November 2020. Piscataway: IEEE, 2020, pp. 1–5.
2. **A. Korneyev**, M. Gorobetz, A. Levchenkov, Unified Energy Efficient Control Algorithm for Electric Unmanned Aerial Vehicles with Different Traction Drives and Configurations. 2018 IEEE 59th International Scientific Conference on Power and Electrical Engineering of Riga Technical University (RTUCON 2018), Latvia, Riga, 12–14 November 2018. Piscataway: IEEE, 2018, pp. 537–542.
3. **A. Korneyev**, M. Gorobetz, I. Alps, L. Ribickis. Adaptive Traction Drive Control Algorithm for Electrical Energy Consumption Minimisation of Autonomous Unmanned Aerial Vehicle. /Electrical, Control and Communication Engineering, 2019, Vol. 15, No. 2, pp. 62–70.
4. M. Gorobetz, A. Potapovs, **A. Korneyev**, Analysis and Modelling of UAV Electrical Traction Drive based on Empirical Data for Energy Efficiency Tasks. 2019 IEEE 60th International Scientific Conference on Power and Electrical Engineering of Riga Technical University (RTUCON 2019), Latvia, Riga, 7–9 October 2019. Piscataway: IEEE, 2019, pp. 399–403.
5. M. Gorobetz, A. Potapovs, **A. Korneyev**, I. Alps. Device and Algorithm for Vehicle Detection and Traffic Intensity Analysis //Electrical, Control and Communication Engineering, 2021, Vol. 17, No. 1, pp. 83–92.
6. M. Gorobetz, L. Ribickis. A. Beinarovica, A. Kornejevs, Immune Neural Network Machine Learning of Autonomous Drones for Energy Efficiency and Collision Prevention. Drones – Various Applications, Rijeka, Published: September 18, 2023, doi:10.5772/intechopen.1002533
7. E. Kamolins, M. Gorobetz, K. Malnaca, **A. Korneyev**. Analysis of Test Results for Developed Technology of Diesel Bus Conversion into Electric Bus. Reliability and Statistics in Transportation and Communication, Cham: Springer Nature Switzerland AG 2019, 2020. Pp. 1–10.
8. M. Gorobetz, **A. Korneyev**, L. Zemite. Long-term Energy and Fuel Consumption Forecast in Private and Commercial Transport using Artificial Life Approach. ENERGYCON 2022: 7th IEEE International Energy Conference, Latvia, Riga, 9–12 May 2022. Piscataway: IEEE, 2022, pp. 1–6.
9. M. Gorobetz, L. Zemite, A. Jasevics, **A. Korneyev**. Intelligent Algorithm for Using Overall Energy Consumption Statistics. 2020 IEEE 61st International Scientific Conference on Power and Electrical Engineering of Riga Technical University (RTUCON 2020), Latvia, Riga, 5–7 November 2020. Piscataway: IEEE, 2020, pp. 1–13.
10. Malnaca, K., Gorobetz, M., Yatskiv (Jackiva), I., **Korneyev, A**. Decision-Making Process for Choosing Technology of Diesel Bus Conversion into Electric Bus. In: Reliability and Statistics in Transportation and Communication: Selected Papers from the 18th International Conference on Reliability and Statistics in Transportation and Communication, RelStat '18. Lecture Notes in Networks and Systems. Vol. 68. Cham: Springer Nature, 2019, pp. 91–102.

Introduction

Deep analysis of the research base reveals that currently, the majority of energy-saving solutions are related to route calculation and trajectory planning for unmanned vehicles, as well as energy-saving algorithms for other equipment unrelated to unmanned vehicle electric propulsion systems. Only a few studies focused on reducing energy consumption explore the mechanical and electrical properties of power devices.

In the context of this research, an **unmanned vehicle** corresponds to an **autonomous electrical vehicle (UV)** that includes an autopilot in its control structure, enabling the control of the vehicle to reach predetermined coordinates.

1. Control structure and description of elements

Detection of control signals for optimizing transportation vehicles. In the context of this research, an unmanned electrical vehicle corresponds to an autonomous vehicle that includes an electric drive and an autopilot in its control structure, enabling the control of the vehicle to reach predetermined coordinates.

To identify the control signals for optimizing transportation vehicles, let us consider the existing types of vehicles based on degrees of freedom and the control signals they employ, assuming that all of them can be unmanned.

Types of transportation based on the mode of movement, for example:

- **water-based –** surface vessels, submarines;
- **air-based –** airplanes, helicopters, multicopters (aerial vehicles with three or more lifting rotors);
- **land-based –** trains, automobiles.

The minimum number of control signals are be present in a train – one control signal. The maximum number of control signals are in a multirotor rotorcraft with wings – four control signals.

Thus, for controlling any transportation vehicle, the maximum number of control signals is four:

c_1 – a roll (aileron) control signal;

c_2 – a pitch (elevator) control signal;

c_3 – a throttle control signal;

c_4 – a yaw (rudder) control signal.

Structure of an unmanned vehicle control. The simplified control structure [33], [36] of UV's control system consists of an input block, route planner, navigation equipment, sensors, autopilot controller, and electric drive [30].

The proposed structure of UVs. To achieve energy-efficient control, it is proposed to integrate a self-learning optimization controller [32], as investigated in this study, into the existing structure of UV control system between the autopilot controller and the electric drive [23], [25]. The proposed scheme for incorporating the self-learning optimization controller into the existing structure of UV control system is depicted in Fig. 1.1.

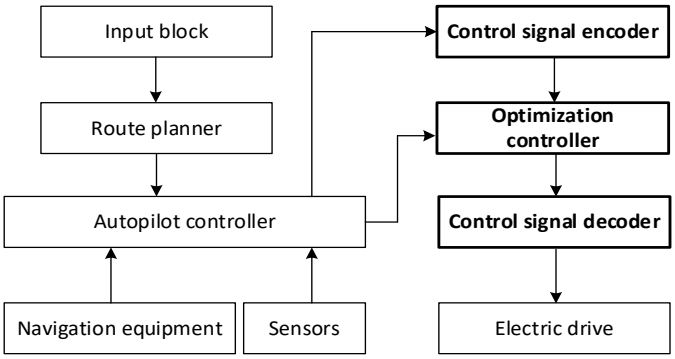

Fig. 1.1. The proposed scheme for integrating the self-learning optimization controller into the existing structure of UVs control system.

Thus, the author proposes to integrate the new optimization controller and the control signal encoder and decoder into the existing control structure of unmanned vehicles. The existing control structure in general consists of an electric drive, sensors, navigation equipment, input data block, a route planner, and an autopilot controller.

The encoder and decoder for control signal components are not considered in this research.

Structure of the self-learning optimization controller. The structural diagram of the self-learning [34], [37] optimization controller (OC) [40] is depicted in Fig. 1.2.

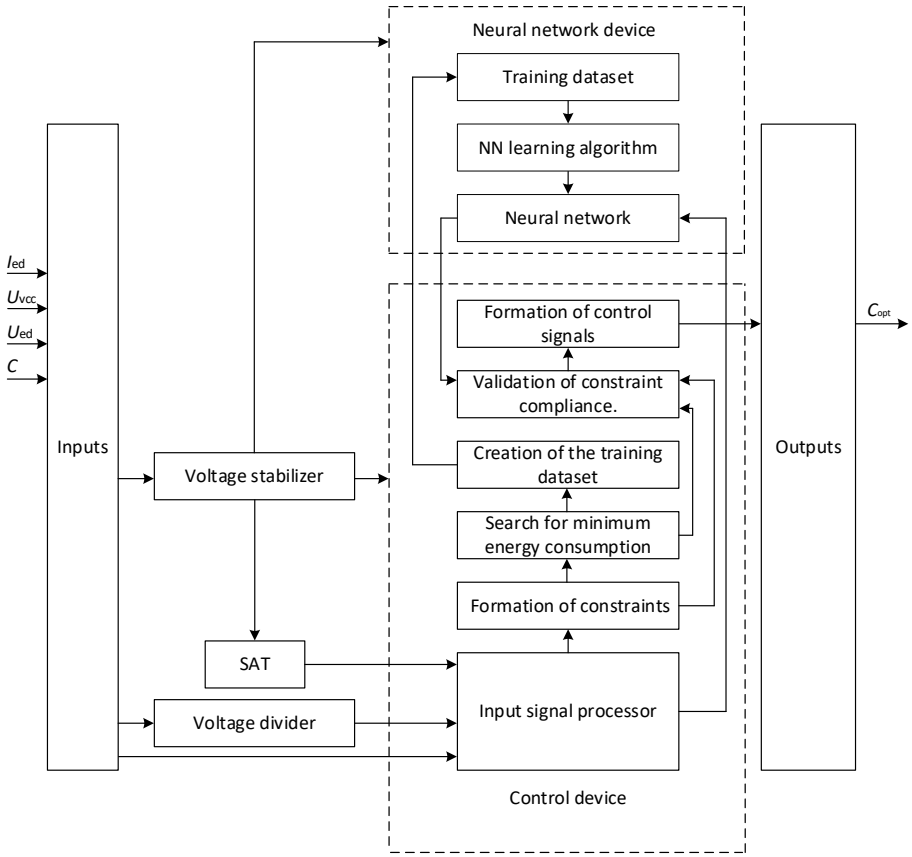

Fig. 1.2. Structural diagram of the self-learning optimization controller.

The structure of the optimization controller consists of inputs, voltage stabilizer, voltage divider, satellite navigation module, neural network (NN) device, control device, and outputs. The voltage and current values of the electric drive [28], [29] and control signals are supplied to the input of the optimization microcontroller. The voltage stabilizer powers the neural network device [26] and the control device. The neural network device implements the neural network [44] and the known neural network training algorithm (for example backpropagation algorithm) and also stores the training dataset. The developed algorithm of the control device includes the algorithm for minimum energy consumption search. For this search, known algorithms (for example, uniform search algorithm) may be applied. Additionally, the newly developed algorithm creates a training data set and generates control signals. The control signals are formed taking into account the constraints imposed by safety and other criteria. The optimized control signals are provided at the outputs. The blocks related to constraints are not considered in this study.

The electrical scheme of the self-learning optimization controller. The electrical diagram [42] of the self-learning optimization controller for optimal energy-efficient control [41] is depicted in Fig. 1.3.

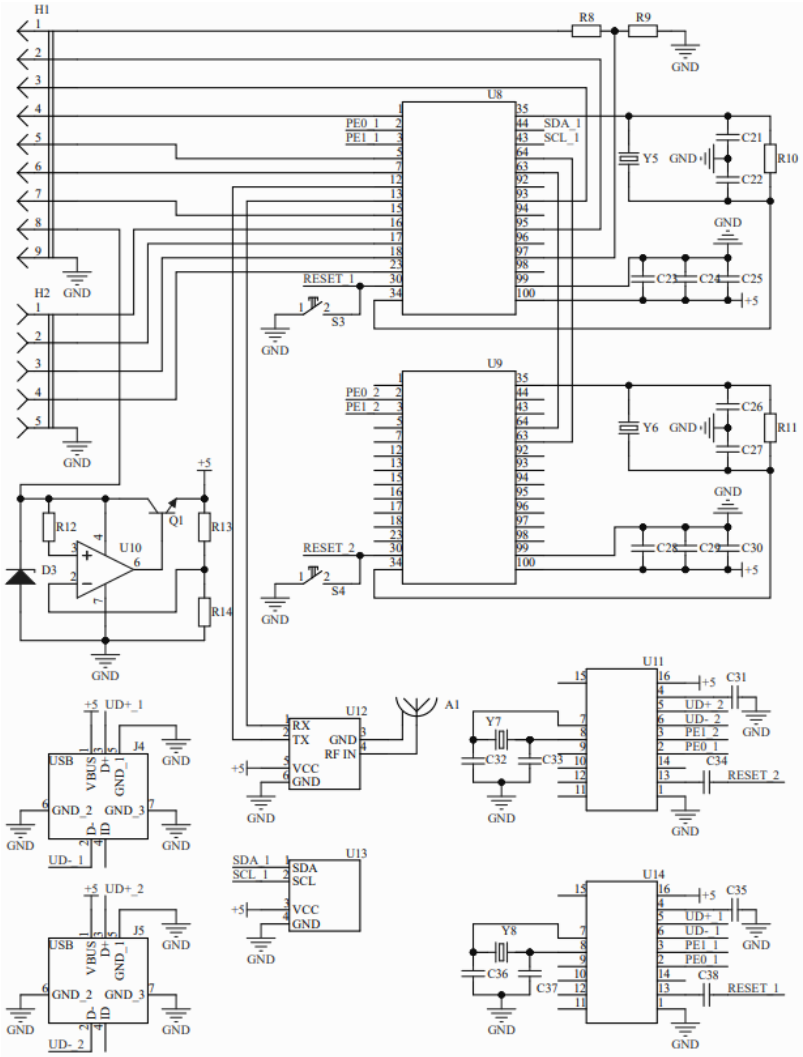

Fig. 1.3. Electrical scheme of the self-learning optimization controller.

In the electrical scheme of a self-learning optimization controller, contact 1 of connector H1 is connected to a voltage divider consisting of resistors R1/R2. The contact number 8 is connected to a voltage stabilizer consisting of microchip U3, diode D1, transistor Q1, and resistors R5–R7. Control signals c_1, c_2, c_3, and c_4 are connected to microcontroller U1 through contacts 2–5. Contacts 6 and 7 receive the current and voltage values of the electric drive, respectively. Outputs 1–4 represent the optimal control signal values c_{1opt}, c_{2opt}, c_{3opt}, and c_{4opt}. USB connectors J1 and J2 are used for programming microcontrollers U1 and U2. U4 and U7 are UART/USB protocol converters. U5 is a satellite receiver. U6 is a barometer. S1 and S2 are reset buttons for microcontrollers. Y1, Y2, Y3, and Y4 are quartz crystals for frequency stabilization of the microchips. Capacitors C8, C9, and C10 represent a frequency filter that smoothens power fluctuations.

2. Mathematical models for the self-learning optimal control system

The spatial model of vehicles

The UV with 6 degrees of freedom moves relative to an inertial reference frame fixed to the Earth, with coordinate axes Ox, Oy, and Oz. The Oz axis is directed opposite to the gravitational force vector. The UV has its own coordinate system with the center O located at the center of mass of the vehicle, and the Oxy, Oyz, and Ozy axes are parallel and co-aligned with the axes of the fixed reference frame. The angular position of the vehicle is defined by three angles: φ (roll, rotation around the Oxz axis), θ (pitch, rotation around the Oxy axis), and ψ (yaw, rotation around the Ozy axis), which respectively determine rotations around the axes.
x, y, z – main axes direction of movement.
$\angle\varphi, \angle\theta, \angle\psi$ – vehicle position angles relative to coordinates.
Signals of control required for movement in 3-dimensional space:
c_1 – a roll (aileron) control signal level;
c_2 – a pitch (elevator) control signal level;
c_3 – a throttle control signal level;
c_4 – a yaw (rudder) control signal level.

We assume that the motion occurs in the xy, xz, and yz planes. The angles ∠φ, ∠θ, and ∠ψ are formed by displacements in these planes. To control any UV, four control signals are sufficient. Thus, the minimum number of control signals for a train is one, while the maximum number is four, for a multirotor aircraft with variable-pitch propellers.

Definition of the target function

The primary criterion of the target function is UV energy consumption minimization, which in general form is represented as the following equation:

$$E = f_1(C, Q) \rightarrow \min \tag{2.1}$$

The secondary criterion is a minimization of the maneuver time that should be minimal in the case when the primary criterion is satisfied, i.e., if more than one solution exists with the same minimal energy consumption, then the maneuver with the shortest time should be selected:

$$\tau = f_2(C) \rightarrow \min, \tag{2.2}$$

where
E – electrical energy consumption for the maneuver completion, Ws;
C – a set of adaptive control parameters, i.e., $C = (c_1, c_2, c_3, c_4)$;
Q – an uncontrollable parameter set, internal, external and environmental impacts;
τ – time spent for maneuver, s.
Start parameters: $c_1 = 0$, $c_2 = 0$, $c_3 = 0$, $c_4 = 0$, $az(R)$ 0°, $targ = 0 + n$.

$$\begin{cases} E_v = \int I \cdot U \cdot \mathrm{d}t = f\,(\mathrm{c}_1, \mathrm{c}_2, \mathrm{c}_3, c_4, t) \rightarrow \min \\ |az(c_4) - targ| \rightarrow 0 \\ |x(c_1, c_2) - x_M| \rightarrow 0 \\ |y(c_1, c_2) - y_M| \rightarrow 0 \\ |z(c_3) - z_M| \rightarrow 0 \\ c_{1min} \le c_1 \le c_{1max} \\ c_{2min} \le c_2 \le c_{2max} \\ c_{3min} \le c_3 \le c_{3max} \\ c_{4min} \le c_4 \le c_{4max} \end{cases}. \tag{2.3}$$

In the present study, the maneuver means the achievement of the target point M (x_M, y_M, z_M) from the current UV location S (x_0, y_0, z_0), within the condition:

$$\begin{cases} |x_{\mathrm{M}} - x_0| \le \varepsilon_X \\ |y_{\mathrm{M}} - y_0| \le \varepsilon_Y \\ |z_{\mathrm{M}} - z_0| \le \varepsilon_Z \end{cases}, \quad (2.4)$$

where

$\varepsilon_{\mathrm{X}}, \varepsilon_{\mathrm{Y}}, \varepsilon_{\mathrm{Z}}$ – an acceptable precision by O_x, O_y, O_z axes.

The definition of the power consumption function

The total electricity consumption [35] of the UV can be determined as follows:

$$E = \int_0^{\tau} u(t, c(t)) \cdot i(t, c(t)) \cdot \mathrm{d}t = E_v + E_p. \quad (2.5)$$

Energy consumption of UV in continuous form is the following:

$$E_v = \int_0^{\tau} \sum_{j=1}^{\mathrm{N}} u_j(t, c(t)) \cdot i_j(t, c(t)) \cdot \mathrm{d}t. \quad (2.6)$$

The electricity consumption of other equipment can be determined as follows:

$$E_{\mathrm{p}} = E - E_{\mathrm{v}}, \quad (2.7)$$

where

E – total energy consumption expenditure during maneuver, Ws;
E_{v} – consumed energy by traction drives for maneuver, Ws;
E_{p} – energy consumed by other electrical equipment for the maneuver, Ws;
t – momentary time values, s;
τ – maneuver completion time, s;
$c(t)$ – a set of momentary control signal values, μs;
N – the number of UV traction drives (traction motor and electronic speed controllers);
j – an index of UV traction drive;
$u_j(t)$ – a momentary voltage value of j-th traction drive, V;
$i_j(t)$ – a momentary current value of j-th traction drive, A;
$u(t)$ – the battery voltage of the UV at time t is denoted as V;
$i(t)$ – the battery current of the UV at time t is denoted as A.

In discrete [51] form, the energy consumption of UV can be determined as follows:

$$E = \sum_{t=0}^{\tau} P_t \mathrm{d}t = \sum_{t=0}^{\tau} (u_t \cdot i_t) dt \,/3600, \quad (2.8)$$

where

dt – discrete time step, in seconds, s;
P_t – instantaneous power, Wh;
u_t – measured voltage, V;
i_t – measured current, A.

When solving the problem, we assume that the design and equipment of the UV comply with the conditions of electrical equipment coordination:

- the output voltage of the battery pack and the maximum output current correspond to the current and voltage of traction motors and electronic speed controllers;
- the maximum values of peak and continuous current for electronic speed controllers correspond to the current of traction motors.

Development of a mathematical model for calculating the motion of an UV

In this section, a mathematical model for the motion of the UV is being created. It will allow simulating its movement in space and calculating the energy consumption.

The model is based on the fundamental law of classical mechanics, actually Newton's second law of motion:

$$F_{\mathrm{vil}} - F_{\mathrm{gr}} - F_{\mathrm{ga}} = m \cdot a, \quad (2.9)$$

where
F_{vil} – UV resultant force, N;
F_{ga} – resistance force, N;
F_{gr} – gravity force, N;
m – UV mass, kg;
a – UV acceleration, m/s^2.

Figure 2.1 shows the vectors of these forces.

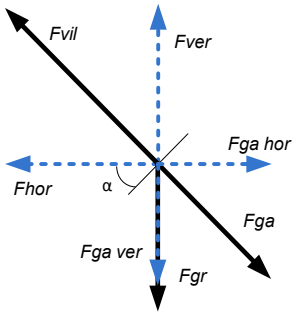

Fig. 2.1. Forces acting on the UV.

Distribution of forces into vertical and horizontal components:
F_{ver} – vertical lift force of the UV, N;
F_{hor} – horizontal lift force of the UV, N.

$$F_{ga} = \rho \cdot C_D \cdot A_{eff} \cdot v^2. \quad (2.10)$$

$$F_{gr} = m \cdot g_0 . \quad (2.11)$$

UV acceleration is calculated from the force equation:

$$a = \frac{F_{vil} - F_{gr} - F_{ga}}{m}. \quad (2.12)$$

UV velocity:

$$v = \int_0^\tau a \, dt. \quad (2.13)$$

UV distance:

$$s = \int_0^\tau v \, dt. \quad (2.14)$$

Mechanical power (instantaneous):

$$N_{(t)} = F_t \cdot v(t). \quad (2.15)$$

The following functional dependencies are defined for the UV velocity limits.
Maximum vertical velocity [24]:

$$V_{ver} = \sqrt{\frac{2 \cdot m \cdot g_0}{\rho \cdot C_D \cdot A_{eff}}} * \sqrt{(FR - 1)} . \quad (2.16)$$

Maximum horizontal velocity:

$$V_{hor} = \sqrt[4]{1 - \frac{1}{FR^2}} \cdot \sqrt{\frac{2 \cdot m \cdot g_0}{\rho * C_D \cdot A_{eff}}} \quad (2.17)$$

$$FR = \frac{F}{m \cdot g_0}, \quad (2.18)$$

where:
F – motor summary traction power, N;
g_0 – gravity acceleration value 9.81 m/s^2;
C_D – aerodynamic flow factor;

A_{eff} – UV effective area, m^2;
ρ – air density, кg/m^3.

Electromechanical models of electric unmanned vehicles

Mechanical model [6] of the UV defined by following parameters:

- m – mass of UV, kg;
- $A^{\text{hor}}_{\text{eff}}$ – area of the UV in horizontal plane, m$^{2;}$
- $A^{\text{ver}}_{\text{eff}}$ – area of the UV in horizontal plane, m$^{2;}$
- F_{t} – summarized traction force, N;
- x, y, z – translational position in the space, where z is vertical axis, m;
- φ, θ, ψ – angles of UV rotational position in the space, rad;
- a_{ver} – vertical acceleration of the UV, m/s^2
- a_{hor} – horizontal acceleration of the UV, m/s^2
- v_{ver} – vertical speed of the UV, m/s;
- v_{hor} – horizontal speed of the UV, m/s.

Battery parameters:

- C_{bat} – capacity of the battery, Ah;
- I_{bat} – relative maximal current, A;
- N_{bat} – number of battery cells;
- U_0 – battery momentary voltage without load, V.

Motor drive control parameter:

- $PW = \{PW_1 \ldots PW_{\text{n}}\}$ – set of pulse widths for each motor, μs.

Motor parameters:

- P_{nom} – nominal power, W;
- $F^j{}_t$ – traction force of each j-th motor, N;
- $I^j(U_{\text{unload}}, F^j{}_t)$ – momentary current of the j-th motor with given traction force, A;
- $P^j(U_{\text{unload}}, F^j{}_t)$ – momentary power of the j-th motor with given traction force, W;
- $U^j{}_{\text{load}} = P^j/I^j$ – momentary voltage of the j-th motor with the given traction force, V.

Approximated functions for motor current and power in the following form of second-order polynomial by obtaining empirical data:

$$I^j\left(U_0, F_t^j\right) = \alpha_i(U_0) \cdot \left(F_t^j\right)^2 + \beta_i(\text{U}_0) \cdot F_t^j + \gamma_i(U_0) \tag{2.19}$$

$$P^j\left(\text{U}_0, F_t^j\right) = \alpha_{\text{p}}(U_0) \cdot \left(F_t^j\right)^2 + \beta_{\text{p}}(U_0) \cdot F_{\text{t}}^{\text{j}} + \gamma_{\text{p}}(\text{U}_0). \tag{2.20}$$

where each coefficient is a linear function:

$$\alpha_i(U_0) = \kappa_{\text{i}}^{\alpha} \cdot U_{\text{unload}} + \delta_{\text{i}}^{\alpha}; \tag{2.21}$$

$$\beta_i(U_0) = \kappa_{\text{i}}^{\beta} \cdot U_{\text{unload}} + \delta_{\text{i}}^{\beta} \tag{2.22}$$

$$\gamma_i(U_0) = \kappa_{\text{i}}^{\gamma} \cdot U_{\text{unload}} + \delta_{\text{i}}^{\gamma} \tag{2.23}$$

$$\alpha_{\text{p}}(U_0) = \kappa_{\text{p}}^{\alpha} \cdot U_{\text{unload}} + \delta_{\text{p}}^{\alpha} \tag{2.24}$$

$$\beta_{\text{p}}(U_0) = \kappa_{\text{p}}^{\beta} \cdot U_{\text{unload}} + \delta_{\text{p}}^{\beta} \tag{2.25}$$

$$\gamma_{\mathrm{p}}(U_0) = \kappa_{\mathrm{p}}^{\gamma} \cdot \mathrm{U}_{\mathrm{unload}} + \delta_{\mathrm{p}}^{\gamma}. \quad (2.26)$$

For UV movement simulation forces are calculated by following equations:

$$F_{\mathrm{t}} = \sum_{j=1}^{\mathrm{n}} F_t^j \quad (2.27)$$

$$F_{\mathrm{z}} = F_{\mathrm{ver}} = F_{\mathrm{t}} \cdot \cos\varphi \cos\theta \quad (2.28)$$

$$F_{\mathrm{hor}} = \sqrt{(F_{\mathrm{t}})^2 - (F_{\mathrm{ver}})^2} \quad (2.29)$$

$$F_{\mathrm{x}} = F_{\mathrm{hor}} \cdot \cos\psi \sin\varphi \cos\theta + \sin\psi \sin\theta \quad (2.30)$$

$$F_{\mathrm{y}} = F_{\mathrm{hor}} \cdot \sin\psi \sin\varphi \cos\theta - \cos\psi \sin\theta \quad (2.31)$$

$$F_{\mathrm{g}} = m \cdot g \quad (2.32)$$

$$F_{\mathrm{res}}^{\mathrm{ver}} = \rho \cdot c_{\mathrm{d}} \cdot A_{\mathrm{eff}}^{\mathrm{ver}} \cdot (v_{\mathrm{ver}})^2 \quad (2.33)$$

$$F_{\mathrm{res}}^{\mathrm{hor}} = \rho \cdot c_{\mathrm{d}} \cdot A_{\mathrm{eff}}^{\mathrm{hor}} \cdot (v_{\mathrm{hor}})^2, \quad (2.34)$$

where

g = 9.81 – the Earth's gravity constant, m/s^2;

ρ = 1.2255 – air density assumed as a constant, kg/m^3.

For UV hovering the following condition should be satisfied:

$$F_{\mathrm{ver}} = F_{\mathrm{g}}, F_{\mathrm{hor}} = 0. \quad (2.35)$$

For UV vertical lift up the following condition should be satisfied:

$$F_{\mathrm{ver}} > F_{\mathrm{g}}, F_{\mathrm{hor}} = 0. \quad (2.36)$$

For UV horizontal movement on the constant altitude the following condition should be satisfied:

$$F_{\mathrm{ver}} = F_{\mathrm{g}}, F_{\mathrm{hor}} > 0. \quad (2.37)$$

Energy consumption in Wh and battery capacity consumption in Ah is calculated by the following equations:

$$E_{\mathrm{cons}} = \int_0^{\tau} \left(\sum_{j=1}^{\mathrm{n}} P^j \left(U_0, F_{\mathrm{t}}^{\mathrm{j}} \right) \right) \mathrm{d}t \quad (2.38)$$

$$C_{\mathrm{cons}} = \int_0^{\tau} \left(\sum_{j=1}^{\mathrm{n}} \frac{I^{\mathrm{j}}\left(U_0, F_{\mathrm{t}}^{\mathrm{j}} \right)}{3600} \right) \mathrm{d}t, \quad (2.39)$$

where τ – time moment

Mechanical power (instantaneous):

$$N_{(\mathrm{t})} = F_{\mathrm{t}} \cdot v(t). \quad (2.40)$$

Mechanical work:

$$A = \int_0^{\tau} N \cdot \mathrm{d}t \,/3600. \quad (2.41)$$

Power consumption:

$$P = U \cdot I. \quad (2.42)$$

Torque on the motor shaft:

$$M_{\mathrm{sl}} = 9950 \frac{P}{n}. \quad (2.43)$$

Efficiency of UV:

$$\eta = \frac{\sum A}{\sum E}. \quad (2.44)$$

Mathematical model of a neural network

Neural network notations. Let us define the following designations in neural network models [31], [24]:

t – time moments;

i, j, k – neural network indices. Neuron j is a neuron in the hidden layer and is located in the layer following layer i, while neuron k is located in the layer following neuron j;

n – iteration corresponding to the n-th training sample;
$In(t)$ – an input signal of m dimensions at time moment t;
$In_i(n)$ – the i-th element of the input vector $X(n)$ in the n-th iteration;
$d(t)$ – scalar system output signal at time moment t;
$y(t)$ – neural network output at time moment t;
$e(t)$ – error, the deviation of the output signal $y(t)$ from the desired signal $d(t)$ at time moment t;
$e_j(n)$ – error of neuron j in the n-th iteration;
$d_j(n)$ – target result of the j-th neuron;
$y_j(n)$ – functional signal of the j-th neuron;
$w_{ji}(n)$ – weight between the i-th neuron in the previous layer and the j-th neuron in the current layer;
$\Delta w_{ji}(n)$ – correction of the weight between the i-th neuron in the previous layer and the j-th neuron in the current layer.;
b_j – bias of the j-th neuron;
$w_{j0} = b_j$ – bias in the form of a weight, with $x_0 = +1$;
$v_j(n)$ – induced local field (weighted sum of all weight-input and bias) of neuron j in the n-th iteration;
$\varphi_j(y_j(n))$ – activation or transfer function of the j-th neuron;
$E(n)$ – current sum of squared errors (error energy) in the n-th iteration;
E_{av} – average error for the entire training set;
∇ – gradient operator;
η – training rate parameter;
k – size of the input layer;
nq – size of the hidden layer;
m – size of the output layer.

General mathematical model for a neural network

Each neuron has an input data vector, weights for each input vector element, an activation function, and an output. A neural network typically consists of multiple layers. Each layer can have a defined or undefined number of neurons. Neural networks [52] enable the analysis of an object based on the input parameter vector and determine the object's affiliation to a specific class. This means that neural networks need to be trained in order to determine the object's affiliation to predefined classes.

The mathematical model of a neural network can be defined as follows:

- neural network input signal vector: $In = \{in_1, in_2, \ldots, in_k\}$;
- set of neurons in the hidden layer: $P = \{p_1, p_2, \ldots, p_{nq}\}$;
- neural network output vector: $c_{opt} = \{c_{opt1}, c_{opt2}, \ldots, c_{optm}\}$;
- set of weight vectors for each input of the i-th neuron in the j-th layer: $W_i^j = \{w_{i1}, w_{i2}, \ldots, w_{in}\}$;
- bias for each i-th neuron in the j-th layer: b_i^j;
- summation function for each i-th neuron in the j-th layer: $s_i^j = \sum(W_i^j \cdot X) + b_i^j$;
- activation function for all neurons in the j-th layer: $F^j(s^j)$.

3. Algorithms for a self-learning optimal control system

UV general optimal control algorithm

All the optimal value search methods discussed in the Thesis are based on comparing the values of two target functions and making the corresponding decisions based on the improvement (success) or deterioration (failure) of the target function value.

UV optimal control algorithm [45], [46] in general form:

Step 1. Generation of initial control signal – specify the value of the control signal.

Step 2. Measurement – measure or calculate the value of the target function.

Step 3. Optimization – apply a specific optimization method to make a decision and execute an action for the next value of the control signal.

Step 4. Checking the reached optimal value – if the optimal value has not been reached, return to step 2 with a new control signal until the optimal control value is achieved, then proceed to step 5.

Step 5. Waiting – after reaching the optimal value, after a certain time, it is necessary to recheck the optimal value because the motion conditions may change, then repeat step 2.

Defining the algorithm in more detail, taking into account the information available from the OC controller and its sensors, the steps of the UV energy consumption minimization algorithm would look as follows:

Step 1. Specify the initial control signal c.

Step 2. Measuring the acceleration a, find the time moment when a < eps ~ 0, then set v = const. Such a transition process is not taken into account.

Step 3. Save the energy consumption value at the given moment as e0, time as t0, and distance as s0.

Step 4. After a fixed time t_f = const, calculate the energy consumption per meter. (Wh/m)

$$de = (e - e_0)/(s - s_0). \tag{3.1}$$

Step 5. If de_1 has not been saved yet, then save $de_1 = de$; otherwise, $de_2 = de$.

Step 6. If de_2 is defined, then proceed to step 7.

Step 7. If $de_2 < de_1$,

a) then, if the current control signal is better than the previous one and movement occurs in an extreme direction and according to the chosen optimization method, the next signal c is generated (in case of an unsuccessful attempt);

b) otherwise, if the current control signal is worse than the previous one and according to the chosen optimization method, the next signal c is generated (in case of an unsuccessful attempt).

Step 8. Check the fulfillment of the condition for reaching the optimal values:

a) if it is completed, then the waiting mode is skipped and the next search for the optimal value will occur after time tg;

b) if the condition is not fulfilled, then proceed to step 2.

The Thesis considers two deterministic and two stochastic methods for further testing and suitability for optimal UV control:

- Uniform search method (deterministic)
- Halving method (deterministic)
- Algorithm with backtracking to unsuccessful step (stochastic)
- Random search method (stochastic)

Uniform search algorithm

Uniform search algorithm [50] is defined for optimization with constraints, and its task is formulated as follows: find the minimum of a one-dimensional unimodal function $\Phi(x)$ defined on a closed interval $D = [a, b]$, $x\epsilon[a, b]$.

$$\min \Phi(X) = \Phi(x^*). \tag{3.2}$$

This algorithm belongs to a group of methods where the main idea is to reduce the uncertainty interval of the search and exclude subintervals from the search process where the point x^* does not exist, taking into account the unimodality of the function $\Phi(x)$.

The current interval with uncertainty is denoted as *TIN*, and its length is represented by | *TIN* |. So, if $TIN = [a, b]$, then $|TIN| = b - a$.

In the uniform search algorithm, attempts are made by uniformly dividing the interval $[a, b]$ into N equal subintervals.

Among the calculated values of the function $\Phi(x)$, the smallest value is chosen. Assume that this value is at the point x_k. Then, taking into account the unimodality of the function $\Phi(x)$, the subintervals $[a, x_{k-1}]$ and $[x_{k+1}, b]$ can be excluded from consideration and the new interval $[x_{k-1},\ x_{k+1}]$ is chosen (Fig. 3.1). The algorithm refers to passive search methods. In the uniform search algorithm, attempts are made by dividing the interval $[a, b]$ into N equal subintervals. The minimum value is chosen from the computed values of the function $\Phi(x)$. Let us assume that this value is found at point x_{k}. Then, considering the unimodality of the function x_{k}, the subintervals $[a, x_{k-1}]$ and $[x_{k+1}, b]$ can be excluded from consideration, and the new interval $[x_{k-1},\ x_{k+1}]$ is selected (Fig. 3.1). The algorithm belongs to passive search methods.

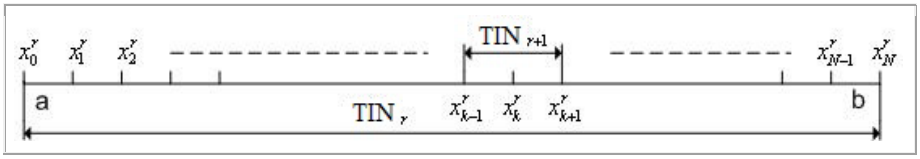

Fig. 3.1. Partitioning of the current interval of uncertainty and defining a new reduced interval.

Any point from the current interval of uncertainty found can be considered as an approximate minimum point x^* with equal conditions.

Algorithm with the halving method

The halving method [50] is also defined for optimization with conditions, and its task is formulated as follows: find the minimum of a unimodal function $\Phi(x)$ in a closed interval $D = [a, b]$.

In the halving method, also known as the uniform dichotomous search algorithm, attempts are made in pairs. The coordinates of each pair differ from the coordinates of another pair by a certain magnitude.

$$\delta_{\text{x}} < \varepsilon_{\text{x}}, \tag{3.3}$$

where ε_{x} – the required accuracy of the solution.

An attempt is made within the TIN. After obtaining the values of the function $\Phi(x)$ at these points, a portion of the *TIN* is excluded from the search due to its unimodality. The size δ_{x} is determined by the required solution accuracy. The algorithm belongs to the class of sequential search methods.

Mathematically, the algorithm can be described by the following scheme:

Step 1. Performs the assignment $r = 1$, $a^1 = a,\ b^1 = b, TIN_1 = [a^1,\ b^1]$.

Step 2. Calculates the values

$$x_0^{\mathrm{r}} = \frac{a^{\mathrm{r}} - b^{\mathrm{r}}}{2}, x_1^{\mathrm{r}} = x_0^{\mathrm{r}} - \frac{\delta_{\mathrm{x}}}{2}, x_2^{\mathrm{r}} = x_0^{\mathrm{r}} + \frac{\delta_{\mathrm{x}}}{2}. \quad (3.4)$$

Step 3. Calculates the function $\Phi(x)$ value $\Phi(x_1^r), \Phi(x_2^r)$.

Step 4. If $\Phi(x_1^{\mathrm{r}}) < \Phi(x_2^{\mathrm{r}})$,

then performs the assignments

$$a^{\mathrm{r}+1} = a^r, b^{\mathrm{r}+1} = x_0^r, TIN_{\mathrm{r}+1} = [a^{\mathrm{r}+1}, b^{\mathrm{r}+1}] \quad (3.5)$$

otherwise, performs the assignments.

$$a^{r+1} = x_0^r, \ a^r, b^{\mathrm{r}+1} = b^r, TIN_{\mathrm{r}+1} = [a^{r+1}, b^{\mathrm{r}+1}]. \quad (3.6)$$

Step 5. If $|TIN_{\mathrm{r}+1}| \leq \varepsilon_{\mathrm{x}}$, then the algorithm ends, otherwise, it continues to execute $r = r + 1$ and goes to step 2.

Algorithm with backtracking to unsuccessful step

It is useful to use stochastic search methods for multidimensional unconditional optimization to find the minimum of the optimality criterion $\Phi(x)$, which is defined in the n-dimensional Euclidean space $\mathbb{R}^n$.

For UV control, it is necessary to enter a condition and limit the desired values in the range of allowed control signal values $x = <R, P, T, Y>$, $x \epsilon \mathbb{R}^4$:

$$\min \Phi(x) = \Phi(x^*) = \Phi^* \quad (3.7)$$

$$\begin{cases} a_{\mathrm{R}} \geq R \geq b_{\mathrm{R}} \\ a_{\mathrm{P}} \geq P \geq b_{\mathrm{P}} \\ a_{\mathrm{T}} \geq T \geq b_{\mathrm{T}} \\ a_{\mathrm{Y}} \geq Y \geq b_{\mathrm{Y}} \end{cases} \quad (3.8)$$

When solving the task with a return to the failed attempt [50] (one-step optimization method), the iteration formula is used:

$$x^{\mathrm{r}+1} = x^{\mathrm{r}} + \lambda^{\mathrm{r}} \frac{\psi^{\mathrm{r}}}{\|\psi^{\mathrm{r}}\|}, \quad (3.9)$$

where:

λ^{r}– the step size of the r-th iteration;

$\Psi^{\mathrm{r}} = (\Psi_1^{\mathrm{r}}, \Psi_2^{\mathrm{r}}, \ldots, \Psi_{\mathrm{n}}^{\mathrm{r}})$ – realization of an n-dimensional random vector;

$\|*\|$ – vector norm (numeric value of a vector).

As a search termination condition, one of the traditional iteration termination conditions can be used:

$$\|\mathbf{X}^{r+1} - \mathbf{X}^r\| = \lambda^r \leq \varepsilon_{\mathrm{X}}, \quad (3.10)$$

where ε_{X} – required search precision by X:

$$|\Phi(\mathbf{X}^{r+1}) - \Phi(\mathbf{X}^r)| \leq \varepsilon_{\Phi}, \quad (3.11)$$

where ε_{Φ} – required search precision by Φ.

Repeated random search algorithm

Repeated random search algorithm [50] is also commonly used for multidimensional unconditional optimization in finding the minimum of the optimality criterion $\Phi(x)$ defined in the *n*-dimensional Euclidean space $\mathbb{R}^n$.

But for UV control, it is also necessary to enter conditions and limit the searchable values in the range of allowed control signal values $x = <R, P, T, Y>$, $x \epsilon \mathbb{R}^4$:

$$\min \Phi(x) = \Phi(x^*) = \Phi^* \quad (3.12)$$

$$\begin{cases} a_{\mathrm{R}} \geq R \geq b_{\mathrm{R}} \\ a_{\mathrm{P}} \geq P \geq b_{\mathrm{P}} \\ a_{\mathrm{T}} \geq T \geq b_{\mathrm{T}} \\ a_{\mathrm{Y}} \geq Y \geq b_{\mathrm{Y}} \end{cases}. \tag{3.13}$$

This repeated random search method uses an iteration scheme

$$\mathbf{X}^{r+1}=\mathbf{X}^{r}+\lambda^{r}\boldsymbol{\Delta}^{r}, \tag{3.14}$$

where

λ^{r} – step size in the r-th iteration;

Δ^{r} – $(n \times 1)$ – unit vector, which shows the search direction in the r-th iteration:

$$\boldsymbol{\Delta}^{r}=\left[\beta\frac{\mathbf{S}^{r}}{\|\mathbf{S}^{r}\|}+(1-\beta)\frac{\mathbf{P}^{r}}{\|\mathbf{P}^{r}\|}\right]. \tag{3.15}$$

where

$S^{r}=\gamma S^{r-1}+(1-\gamma)S^{r-2}-$ the "prehistory" vector that started the average search direction from the previous two steps;

$\|*\|-$ vector norm (numeric value of a vector);

$P^{n}-n$-dimensional vector of uniformly distributed random numbers in the interval [0, 1];

$\beta\epsilon$ [0,1] – coefficient, which determined the influence of "prehistory" (determined part) for the choice of the next step;

$\Delta^{r}-$ random component in vector;

$\gamma\epsilon[0,1]-$ coefficient that gives the value of "prehistory" S^{r-1}, S^{r-2} in the vector S^{r};

$\frac{S^{r}}{||S^{r}||}-$ S^{r} direction vector with length 1;

$\frac{P^{r}}{||P^{r}||}-$ P^{r} direction vector with length 1.

As a search termination condition, one of the traditional iteration termination conditions can be used:

$$\|\mathbf{X}^{r+1}-\mathbf{X}^{r}\|=\lambda^{r}\leq\varepsilon_{\mathrm{X}}, \tag{3.16}$$

where ε_{X} – required search precision by X.

$$|\Phi(\mathbf{X}^{r+1})-\Phi(\mathbf{X}^{r})|\leq\varepsilon_{\Phi}, \tag{3.17}$$

where ε_{Φ} – required search precision by Φ.

A neural adaptive filtering algorithm in a general form

The algorithm is intended for a dynamic system whose mathematical characteristics are unknown [22].

Initialization.

Assume that the given sets of labeled input and output data are generated by the system at discrete time intervals:

$x(t)$ – input m-dimensional signal;

$d(t)$ – scalar system output signal;

where

$t = 1, 2, ..., n$;

In this way, the external behavior of the system can be described by the following set of data:

$$T : \{x(t), d(t); \quad t = 1,2,...,n\}, \tag{3.18}$$

where

$$x(t) = \{x_1(t), x_2(t),..., x_m(t)\}. \tag{3.19}$$

Step 1. Filtration procedure.

The output of the neural network is

$$S = \{y(t), e(t)\}, \tag{3.20}$$

where

$y(t)$ – neural network output;

$e(t)$ – offset of the output signal $y(t)$ from $d(t)$.

Step 2. Adaptation procedure.

Given the linearity of the neuron, the output signal $y(t)$ coincides with the induced local field $v(t)$:

$$y(t) = v(t) = \sum_{i=1}^{m} w_i(t) x_i(t) \tag{3.21}$$

in the form of matrices:

$$y(t) = X^T(t) \cdot W(t), \tag{3.22}$$

where

$$W(t) = \{w_1(t), w_2(t),..., w_m(t)\}^T \tag{3.23}$$

$$e(t) = y(t) - d(t). \tag{3.24}$$

Step 3. Evaluation procedure.

Let us consider the continuously differentiable function $E(w)$ that depends on the vector w. The function $E(w)$ represents the elements of the vector w to the set of real views and is the optimality condition for a selected adaptive filtering algorithm of the vector w.

Step 3.1. We must find such a w^* that

$$E(w^*) \le E(w). \tag{3.25}$$

It poses an unconditional optimization problem:

$$E(w) \to \min \tag{3.26}$$

An optimality condition is required:

$$\nabla E(w^*) = 0. \tag{3.27}$$

Step 3.2. Calculate $\nabla E(w)$,

where ∇ – gradient operator;

$$\nabla = \left[\frac{\partial}{\partial w_1}, \frac{\partial}{\partial w_2}, ..., \frac{\partial}{\partial w_m} \right]^T \tag{3.28}$$

$$\text{but } \nabla E(w) = \left[\frac{\partial E}{\partial w_1}, \frac{\partial E}{\partial w_2}, ..., \frac{\partial E}{\partial w_m} \right]^T. \tag{3.29}$$

Step 4. The correction of the weights takes place in the direction of decreasing the function of the maximum value, opposite to the gradient vector:

$$w(n+1) = w(n) - \eta g(n), \tag{3.30}$$

where

η – positive constant, training rate parameter;

$g(n)$ – gradient vector at point $w(n)$.

Step 5. Weight correction calculation. When moving from the n-th iteration to the $n + 1$ iteration, the algorithm performs the correction of the weight coefficients:

$$\Delta w(n) = w(n+1) - w(n) = -\eta g(n). \tag{3.31}$$

Step 6. Transition to the next iteration to the 1st steps at the condition

$$E(w(n+1)) < E(w(n)), \tag{3.32}$$

where

$w(n)$ – is the previous value of the weight vector;

$w(n + 1)$ – the next value and with $n = n + 1$.

Backpropagation algorithm for neural network training. If a set of training states is given, then we will define the following algorithms for training neural networks.

Algorithm [27] cycles examples from the training set $\{x(n), d(n)\}_{n=1}^{N}$.

Initialization.

The weights $W(0)$ are generated as case numbers with a uniform distribution with mean 0. The variance is chosen so that the standard deviation lies in the linear part of the sigmoid function.

Step 1. Defining the training set.

The training images from the training set – epoch – are passed to the network. Forward propagation and reverse propagation are performed sequentially for each image.

Step 2. Direct propagation of signals.

Let each training image be a pair ($x(n)$, $d(n)$),

where

$x(n)$ – vector of input signals;

$d(n)$ – the target output of the neural network.

Step 3. Computation of weighted sums $v(n)$ and functional signals $\varphi(v(n))$, say from the input layer. The weighted sum for the j-th neuron in the l-th layer is calculated according to the formula:

$$v_j^{(l)}(n) = \sum_{i=0}^{m_0} w_{ji}^{(l)}(n) y_i^{(l-1)}(n), \tag{3.33}$$

where

$y_i^{(l-1)}(n)$ – the output functional signal for the i-th neuron located in the previous layer $l - 1$ in the n-th iteration;

$w_{ji}^{(l)}(n)$ – weight for the connection of the j-th neuron of the l-th layer with the i-th neuron of the $l - 1$ layer.

Step 4. Conditions of direct distribution. If the sigmoid activation function is used, then the output signal for the j-th neuron of the l-th layer is

$$y_j^{(l)}(n) = \varphi_j(v_j(n)). \tag{3.34}$$

If neuron j is in the first layer, at $l = 1$

$$y_j^{(0)}(n) = x_j(n). \tag{3.35}$$

If the neuron is in the output layer, at l = L

$$y_j^{(L)}(n) = o_j(n). \tag{3.36}$$

Step 5. The error is calculated by the formula:

$$e_j(n) = d_j(n) - o_j(n), \tag{3.37}$$

where $d_j(n)$ – the j-th element of the vector $d(n)$.

Step 6. Reverse signal propagation.

Step 7. The local gradients of the nodes are calculated:

$$\delta_j^{(l)}(n) = \begin{cases} e_j^{(L)}(n)\varphi_j'(v_j^{(L)}(n)) \\ \varphi_j'(v_j^{(l)}(n))\sum_k \delta_k^{(l+1)}(n)\delta_{kj}^{(l+1)}(n), \end{cases} \tag{3.38}$$

where $\varphi_j'(n)$ – the derivative of the function by argument.

Step 8. Therefore, the changes in the weights of the l-th layer in training take place according to the delta-law:

$$w_{ji}^{(l)}(n+1) = w_{ji}^{(l)}(n) + \alpha[w_{ji}^{(l)}(n-1)] + \eta\delta_j^{(l)}(n)y_j^{(l-1)}(n), \tag{3.39}$$

where

η – training rate parameter;

α – moment constant.

Step 9. Iterations. The algorithm repeats, returning to step 2, successively applying forward and reverse propagation, cyclically using examples from the epoch, until the stopping criterion is reached.

4. Results of experimental research on developed models and algorithms

Experimental devices

For the research of traction motors, it is necessary to measure the parameters – current, voltage, rotation speed and traction force at set values of the control signal. For this purpose and for computer modeling at work, a frame was made: test bench (Fig. 4.1 a)). To conduct experiments on testing the developed algorithm for optimizing energy consumption with a self-learning neural network, the following devices were made: UAV – unmanned aerial vehicle – quadcopter (Fig. 4.1 b)), and Train – a model of a railroad with an unmanned electric train (Fig. 4.2).

a) b)

Fig. 4.1. a) Test bench; b) UAV.

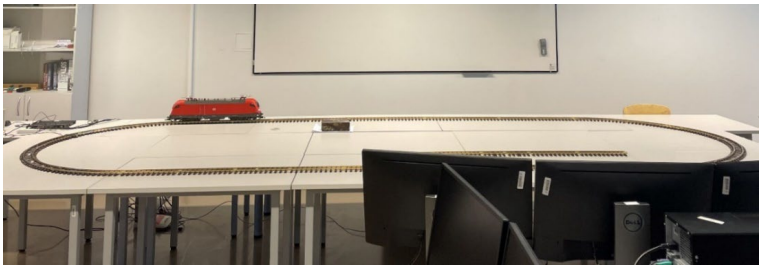

Fig. 4.2. Model of a railroad with an unmanned electric train.

Electrical boards of optimization controller (OC) of UAV are shown in Fig. 4.3 a). The train control board with OC is shown in Fig. 4.3 b).

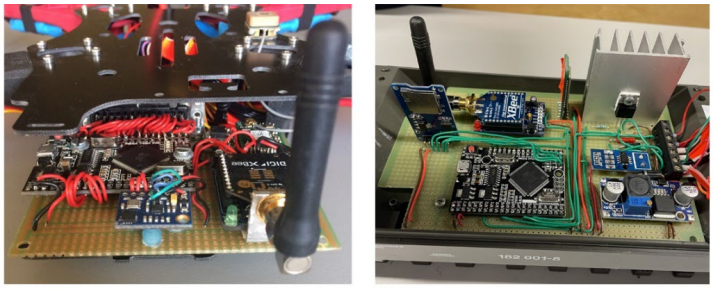

Fig. 4.3. a) Electrical boards OC UAV; b) train control electrical boards with OC.

Electric motors used in experimental devices. Let us take DC brushless motors BR2216-KV810, BR2212-KV920, and BR2212-KV980, which are usually used in amateur quadcopters, and one DC motor without precisely known parameters, let us call it LKD-24 (Fig. 4.4).

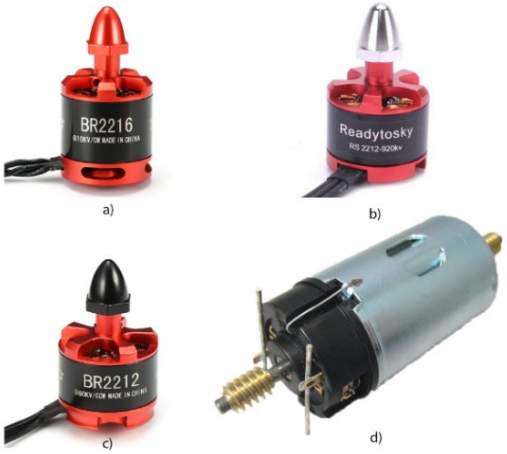

Fig. 4.4. a) BR2216-KV810; b) BR2212-KV920; c) BR2212-KV980; d) LKD-24.

Parameters of electric motors BR2216-KV810, BR2212-KV920, and BR2212-KV980 are shown in Table 1.

Table 1

Parameters Defined by Electric Motor Manufacturers

Motor	**KV** [rpm/V]	**U** [V]	**I** [A]	**F** [g]	**P** [W]	**Eff.** [g/W]	**LiPo** Cell	**m** [g]
BR2216	810	14.8	15.6	1065	231	4.6	2S-4S	66
BR2212	920	11.1	9.5	642	105	6.1	2S-4S	50
BR2212	980	11.1	10.6	710	118	6	2S-4S	50

Device and calibration of an electronic odometer for measuring the distance traveled by a train model. An electronic odometer is made to measure the distance traveled. The odometer mechanism is shown in Fig. 4.5.

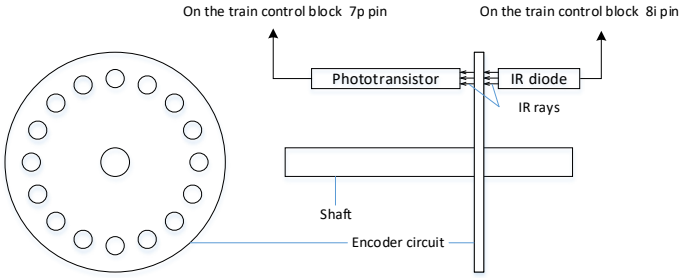

Fig. 4.5. Odometer mechanism.

The infrared diode is supplied with power and emits infrared rays. When rotating the axis on which a transparent coding disk with holes is attached, the microcontroller input is supplied with voltage from the transistor, which varies from 0 volts to 5 volts as the disk moves, passing through transparent and opaque areas. The 10-bit analog-digital converter (ADC) of the microcontroller converts the voltage values into discrete values from 0 to 1024. In the absence of IR radiation, the ADC value is 0, when exposed to IR radiation – 1024. The passage of one transparent and one opaque area is counted as one tact cycle. The passage of the transparent region is considered when the ADC value is greater than 900, followed by the opaque region with an ADC value less than 700. Next, we measure the number of cycles when the train travels the route once. The length of the experimental route is 11 m. To fix one passage, a reed switch is installed on the train, and a permanent magnet is installed on the rails. When traveling 11 m, 800 cycles are recorded. Thus, one odometer cycle is equal to 1.1375 cm.

The control structure of experimental device – quadcopter. The proposed control structure of the UAV consists of the following components. The existing UAV already has flight controller, traction groups with electronic speed controllers ESC and permanent magnet brushless DC motors, accumulator, voltage regulator, radio receiver and built-in sensor components. It is proposed to improve the existing structure by additional optimization controller and additional sensor group containing voltmeter, current meter (hall sensor), accelerometer, barometric altimeter, and satellite positioning module. The radio receiver in the improved structure is used to get the flight goal from the operator to the optimization controller or, in fully autonomous UAV case, the optimization controller is able to define the mission goal by itself (it requires the development of additional decision-making algorithms and is not described in this work).

The control structure of experimental device – train. To monitor the operation of the optimization controller, collect data, and control the startup, a computer [43] with the ARDUINO IDE programming environment is used [48]. The train and the computer exchange data using the Xbee radio module.

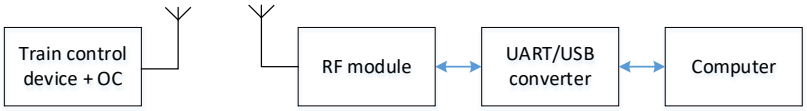

Fig. 4.6. The structure of data exchange between the computer and the train.

The data exchange structure between the computer and the train is shown in Fig. 4.6.

Researching the possibility of optimization

Removal of UAV electric drive characteristics. The thrust force of the motor was measured using a test bench, calculating the force according to the formula:

$$F_{\text{vil}} = m \cdot 9.81, \tag{4.1}$$

where m is measured thrust, kg.

The motor power is calculated as

$$P_{\text{electric drive}} = U \cdot I. \tag{4.2}$$

Since in real conditions the optimisation algorithm does not consider the elements of the electric drive separately but takes into account the total energy consumption, the losses in the wires and the losses in the speed controller are not calculated. Thus, the power consumed by the electric drive consists of

$$P_{\text{electric drive}} = \Delta P_{\text{wire}} + \Delta P_{\text{esc}} + \Delta P_{\text{motor}}, \tag{4.3}$$

where

ΔP_{wire} – power loses in wires;

ΔP_{esc} – power loses in the speed converter;

P_{motor} – motor power (including loses).

Analyzing the minimum function values for different masses, it can be seen that the energy consumption is higher for motors with a higher kV ratio (Fig. 4.7).

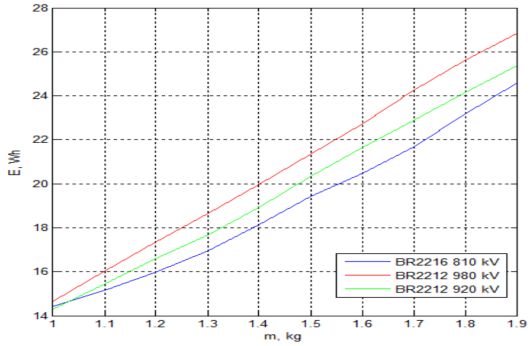

Fig. 4.7. Analysis of the minimum values of the $E(m)$ function for different motors and different UV masses.

Removal of train model electric drive characteristics. The power characteristics of the electric drive on different sections of the road with a constant control signal C = 255 with a train weight of 9.6 kg is shown in Fig. 4.8.

***C* – electric drive control signal using PWM, varying from 0 to 255.**

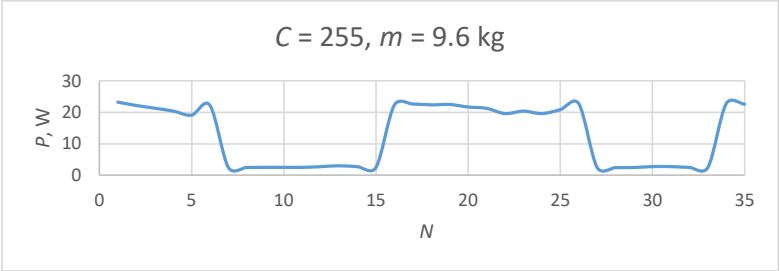

Fig. 4.8. The power characteristics of the electric drive on different sections of the road with a constant control signal $C = 255$ with a train weight of 9.6 kg.

The power characteristics of the electric drive on a straight section of the track under different C control signals, with a train mass of 4.1 kg, is shown in Fig. 4.9.

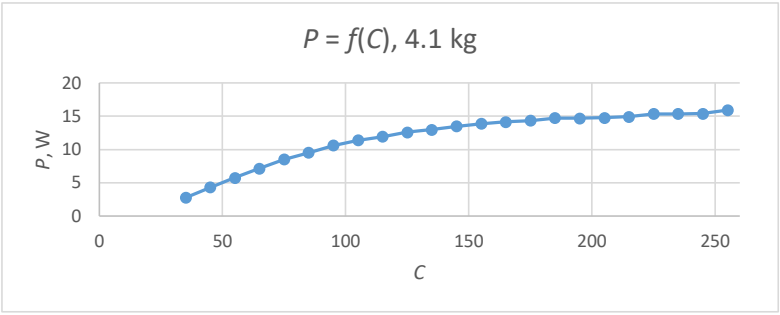

Fig. 4.9. The power characteristics of the electric drive on a straight section of the track under different C control signals, with a train mass of 4.1 kg.

The non-linear nature of the power characteristics of the electric drive under different control signals and the varying power on different sections of the track indicate the potential for energy consumption optimization.

Development of the UV computer model for studying energy consumption minimization target function. The computer model is designed for modeling the vertical motion of a quadcopter [38], [39] towards a specified target point, specifically the target altitude, which is chosen to be sufficient for calculations and further optimization.

Empirical data [47] obtained during the motor research time in the computer model are implemented as a four-dimensional array with the defined number of measurements n: control signal array c, current value array I, voltage value array u, thrust force array f.

To obtain the parameter values between measurements, linear interpolation method is used in the computer model, which, based on the control signal c, allows finding the desired value of another parameter y (current i, voltage u, or force f):

$$y = \frac{(c - c_i)}{(c_{i+1} - c_i)}(y_{i+1} - y_i) + y_i. \quad (4.4)$$

The given parameters for the quadcopter are mass m, effective area A_{eff}, drag coefficient C_d, and air density ρ, which is considered constant at the altitude of the quadcopter (ρ = 1.2255). The first analysis of the target function was performed with varying mass and three different motors: mass ranging from 1 kg to 1.9 kg with a step of 0.1 kg, motors with 810 kV, the constant parameters are $C_d = 1.06$ and $A_{\text{eff}} = 0.25$ m^2.

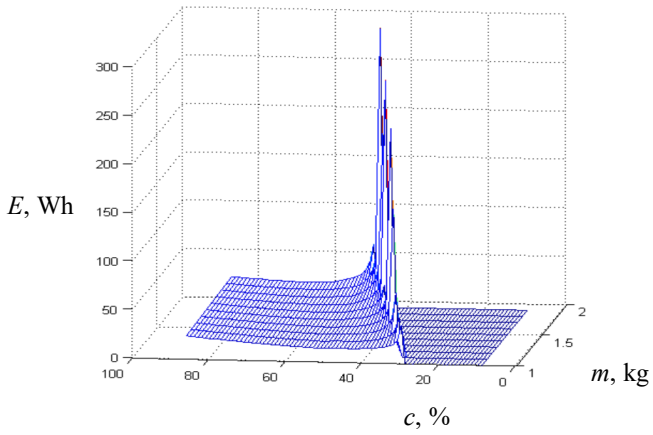

Fig. 4.10. $E(c, m)$ analysis for motors BR2216 810 kV.

In Fig. 4.10, it can be observed that the energy consumption function exhibits a unimodal nature for any given mass and different motors. The only difference lies in the launch thrust control signal required to lift the quadcopter in the air and the value of consumed energy. Therefore, we can conclude that in the study of the target function's dependence on the quadcopter's area and drag coefficient, it is sufficient to evaluate the function for any chosen mass, for example, m = 1.5 kg. Figure 4.11 shows the dependency of the target function E on the effective area A_{eff}, ranging from 0.2 m^2 to 0.4 m^2 with a step of 0.01 m^2.

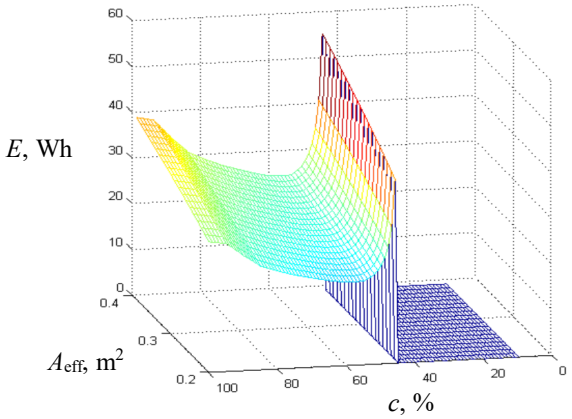

Fig. 4.11. Analysis of the values of the function $E(c, A_{\text{eff}})$.

It can also be seen from the figures that the nature of the function is similar and unimodal and the power consumption increases with increasing effective area and streamline ratio.

Research of the target function of the energy consumption of the train model. To research the target function of energy consumption for the electric train model, let us take a train with different masses of 4.1 kg, 9.6 kg, and 19.3 kg and measure the energy and different control signals in the range from 100 to 255 on a straight section. The measurement results are shown in Fig. 4.12.

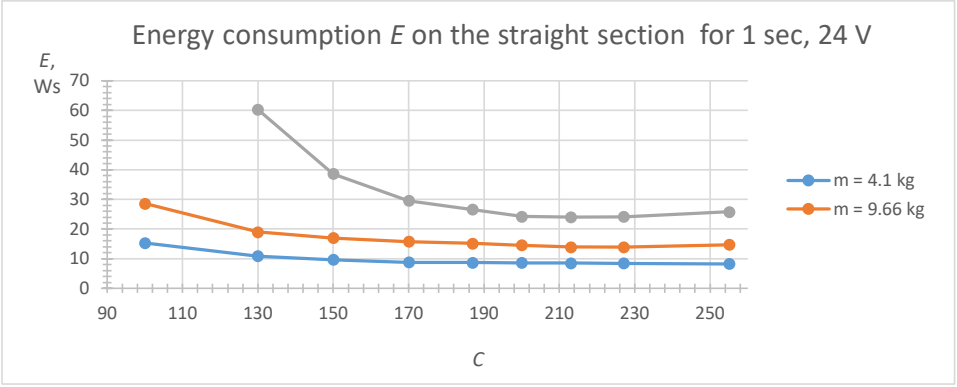

Fig. 4.12. Energy consumption of the electric drive with different control signals and with different masses of the train.

Development of computer models for verification of optimization methods

Searching the optimal control signal for the railway. The search is conducted using a uniform search algorithm with different values of the control signal C step change – from 5 to 30, and a signal change distance ranging from 0.3 meters to 5.5 meters. The table and graphs display the results of the energy consumption measurement experiment using the uniform search algorithm for a combination of C control signal step change of 15 and a signal change distance of 5.5 meters, which demonstrated the lowest energy consumption at a power supply voltage of 24 V. The energy consumption dynamics of an electric train with a constant control signal $C = 255$ and a uniform search algorithm for a distance traveled of 115 meters is shown in Fig. 4.13.

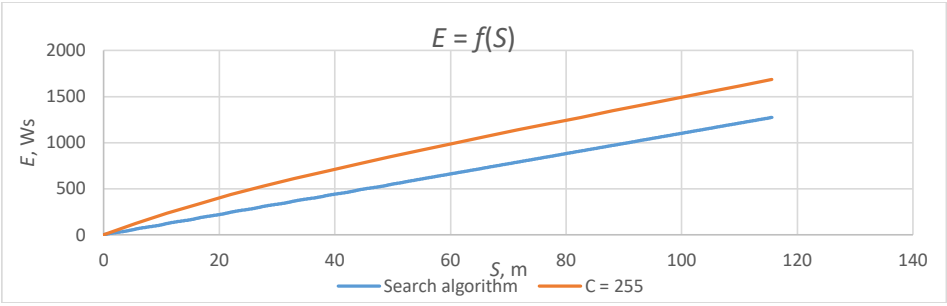

Fig. 4.13. Energy consumption dynamics of an electric train with a constant control signal and $C = 255$ and a uniform search algorithm.

From the dynamics of the control signal graph, it can be observed that the signal gradually increases until reaching its maximum value. However, due to the changing nature of the load, the minimum search algorithm fails to find the optimal control signal. The value of dE/dS decreases with an increase in the control signal value and approaches optimal values. Energy consumption (E) increases with the distance covered. The speed varies depending on the control signal changes and the nature of the load (straight section or turn).

From previous measurements, it is known that a train with a mass of 4.6 kg has the lowest energy consumption for a complete circuit of movement when driven with a constant control signal of $C = 255$, compared to other signals. From the graph, it can be observed that the minimum search algorithm consumes more energy than a single constant signal on all

sections of the path. Therefore, the minimum search algorithm consumes more energy in the search for minimal energy consumption and cannot find the optimal control signal under such load variation.

Based on the experimental results with the train, it is evident that there is no definitive optimal signal, and the search algorithm fails to find it in time. It is necessary for the system to learn to immediately output the required control signal. The proposed solution is a neural network that requires data for training.

Due to legislative restrictions applied to aerial vehicles, experiments with quadcopters are not conducted. Further experiments will be carried out on a train model.

Analysis of data for creating a training set

Estimation of load characteristics for use in a neural network. In this experiment, the energy consumption characteristics were measured for different train masses, with different control signals, and on different sections of the track. Figure 4.14 displays the energy consumption characteristic dE/dS during the train's one complete circuit. The graph includes values with calculated moving averages. Moving averages are used because instantaneous values exhibit significant fluctuations.

Hypothesis: It is possible to assess the load characteristics at each point on the track independently of the control signal and movement speed.

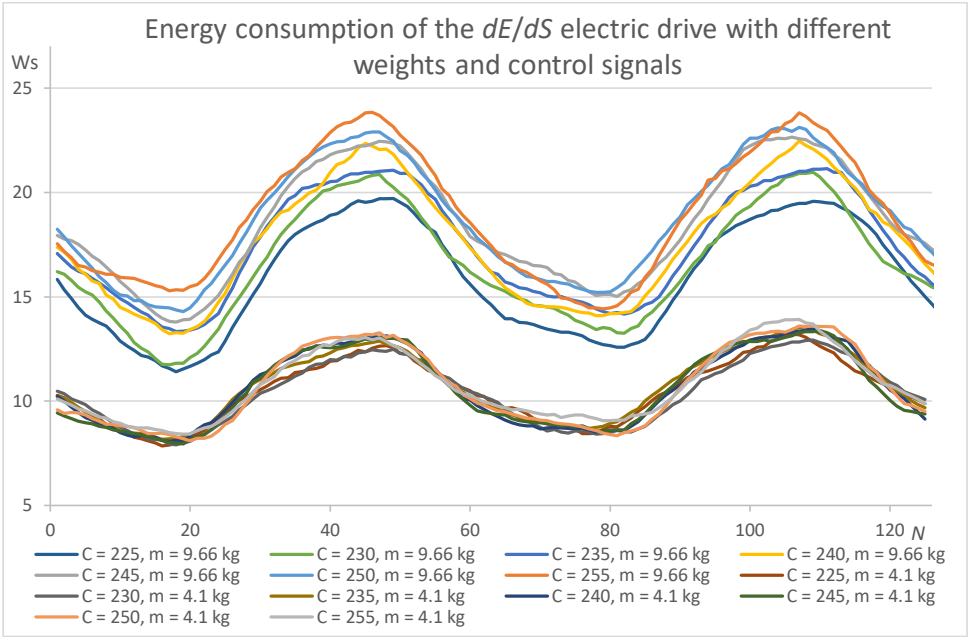

Fig. 4.14. The characteristic of energy consumption dE/dS when the train travels one circle. With train masses m = 4.1 kg and m = 9.6 kg.

It can be seen from the energy consumption graph that for different masses of a train in the same sections, energy consumption will differ.

Let us calculate a value that describes the nature of the load – LC, this will be the last n floating average of the ratio of the current floating average speed V_2 to the previous floating average speed V_1 over the last n samples. The floating average is needed for smoothing. Let us

calculate the *LC* values for a train with a mass of 4.1 kg and 9.6 kg for all sections of the road. In order to see how the nature of the load looks like on different sections of the road, we will build a graph in Fig. 4.15, from the calculated *LC* values for the speed values.

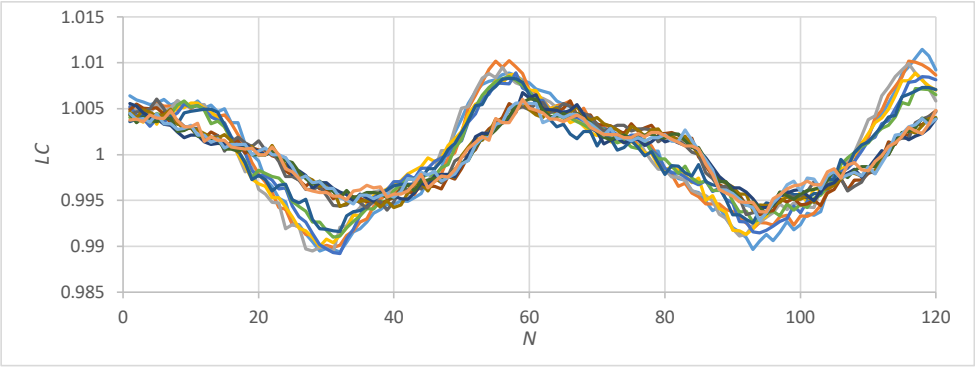

Fig. 4.15. The load characteristics *LC* for a train mass of m = 4.1 kg and m = 9.6 kg.

In the graph, it can be observed that for different masses, the *LC* curves intersect at certain points. During the train's movement, the track may have a negative or positive slope, thereby changing the load as if the train's mass has increased. To differentiate the nature of the effective mass, let us analyze the energy consumption and speed values at all possible sections of the track. When the speed decreases, the *LC* parameter is less than 1, indicating an increased load. Conversely, when the speed increases, the *LC* parameter is greater than 1, indicating a decreased load (with a constant control signal). This value will serve as an auxiliary (primary) element for determining the track section. Thus, the hypothesis that the load characteristics can be assessed at each point on the track independently of the control signal and movement speed is confirmed.

Checking the automatic training set generation algorithm. The train passes through different sections of the track using a single control signal while recording the values of *LC*, speed, control signal, and dE/dS for each section. This process continues until all the new sections are covered. Then, the control signal is increased, and the process described above is repeated. The energy consumption values are also compared, and this process continues until all control signals have been tested and the minimum dE/dS value is found for each section. The control signal corresponding to the minimum dE/dS becomes the optimal signal for that particular section of the track. The obtained values are recorded in the training set.

The dynamics of the control signal *C* are shown in Fig. 4.16. The dynamics of forming the training set *LQ* are shown in Fig. 4.17.

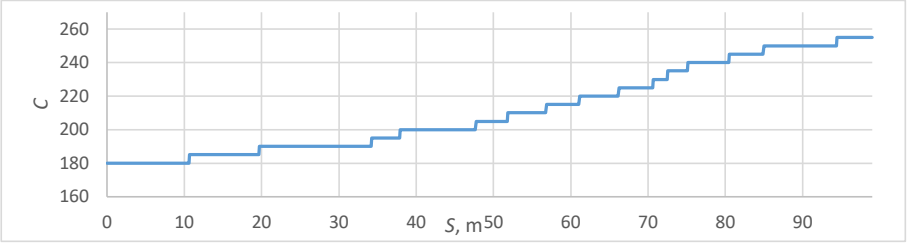

Fig. 4.16. The dynamics of control signal *C* ($C = f(S)$).

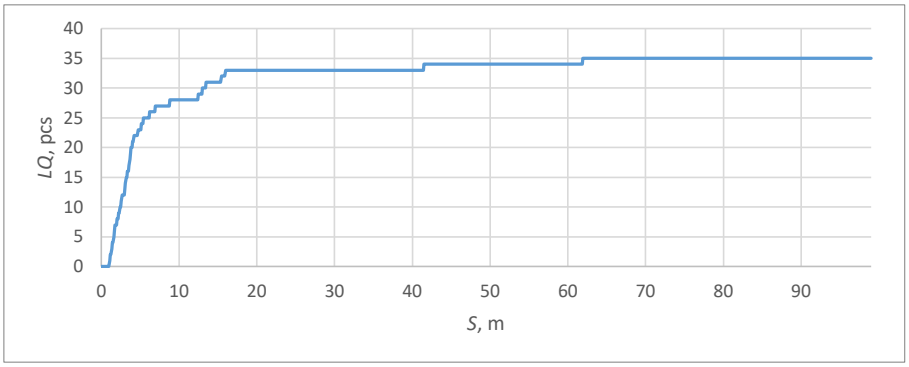

Fig. 4.17. The dynamics of the formation of the training set LQ ($LQ = f(S)$).

The dynamics of the control signal $C = f(S)$ and the quantity of the training set $LQ = f(S)$ show that the train covers different distances at different control signals, i.e., the formation of the training set is not proportional to the distance traveled. Initially, the formation of the training set occurs faster and then slows down. As the control signal increases, there is a trend of decreasing instantaneous energy consumption.

Training set data for neural network training. As a result of the experiment, the automatic training set generation algorithm created a training set for the neural network. The algorithm for automatic creation of a training dataset for the neural network found optimal values of control signals for 35 road sections with varying load characteristics, covering a distance of 62.2 m.

Usage of the complete search algorithm and selection of search parameter settings. Now, using the trained neural network, we will investigate and select the values of dS and the type of velocity input to be used for the neural network – instantaneous or average. To do this, we will conduct a series of experiments with different values of dS in combination with the average velocity and instantaneous velocity, with $U = 28$V.

For each combination, the experiment was repeated 8 times, and the train traveled a distance of 115 m in each experiment. The measurement results are shown in Table 2.

Table 2

Energy Consumption when Operating Different Search Algorithms and a Constant Control Signal at Different Values of dS, Average Speed and Instantaneous Speed at voltage $U = 28$ V

	U = 28 V								
	C_{const}	**Developed self-learning algorithm**							
	-	**V_{avg}**	**V_{mom}**						
dS	-	**0.25**	**0.25**	**0.5**	**1.0**	**1.5**	**2.5**	**3.5**	**5.5**
E_{max}	1420.1	1389.2	1364.0	1376.3	1451.3	1484.8	1475.5	1507.2	1543.3
E_{min}	1410.5	1362.2	1307.2	1345.6	1344.7	1370.9	1396.2	1423.3	1407.0
E_{avg}	1415.3	1372.2	**1335.6**	1361.0	1398.0	1427.8	1435.8	1465.3	1475.1

Designations in the table:

developed algorithm – developed self-learning optimal algorithm with a neural network;
dS – step of energy measurement and control signal C change, m;
V_{mom} – instantaneous value of measured speed, m/s;

V_{avg} – average speed over distance dS, m/s;
E_{min} – the minimum amount of energy consumed to travel 115 m in a series of 8 experiments, Ws;
E_{max} – the maximum amount of energy consumed to travel 115 m in a series of 8 experiments, Ws;
E_{avg} – average energy consumed to travel 115 m in a series of 8 experiments, Ws;
$C_{const} = 255$.

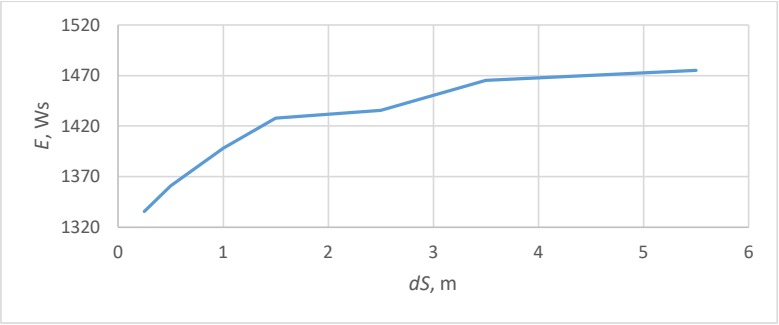

Fig. 4.18. Energy consumption of the train's electric drive depending on the measurement step and changes in the optimization algorithm ($E = f(dS)$).

From the graph in Fig. 4.18, it can be observed that there is a trend of increasing energy consumption with an increase in the measurement step dS. The lowest consumption using the developed algorithm is achieved at 28 volts with $dS = 0.3$ m and using the instantaneous velocity value. It was noticed that the overall energy consumption (relative to the work done) increases when the voltage is set to 28 V compared to 24 V. It was assumed that the motor is designed for a voltage of 24 V, and the decision was made to continue the experiments using the 24 V voltage.

Comparison of the results of the developed self-learning algorithm for optimal energy consumption with a neural network

Below are the results of experiments for a constant control signal C with the lowest energy consumption (in the range from 60 to 255), an algorithm for finding the minimum with the best value based on the results of previous measurements, and a developed algorithm for learning optimal energy consumption using a neural network at a voltage of 24 volts.
In Fig. 4.19, the dynamics of the control signal C are displayed, while Fig. 4.20 shows the dynamics of the train speed. Figure 4.21 depicts the dynamics of dE/dS for the train.

From the dynamics of the control signal graph, it can be observed that the signal quickly reaches the target value and changes according to the load characteristics. The speed V varies depending on changes in the control signal and the load characteristics. The energy consumption E increases with the distance traveled.

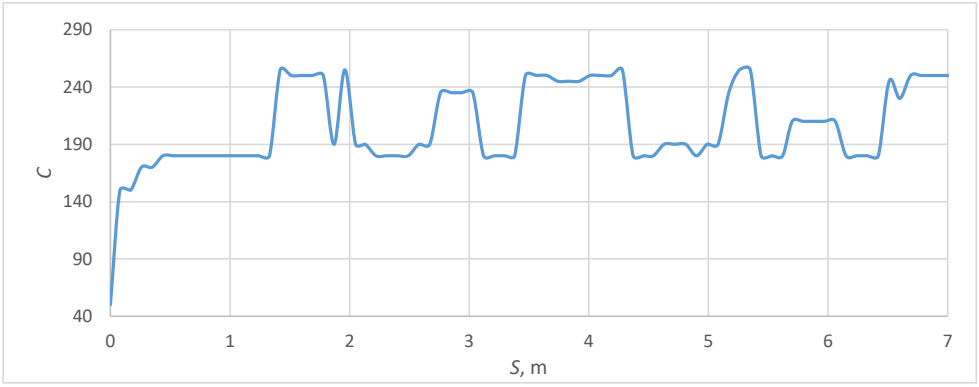

Fig. 4.19. The dynamics of the control signal of the developed algorithm can be observed in the graphs ($C = f(S)$).

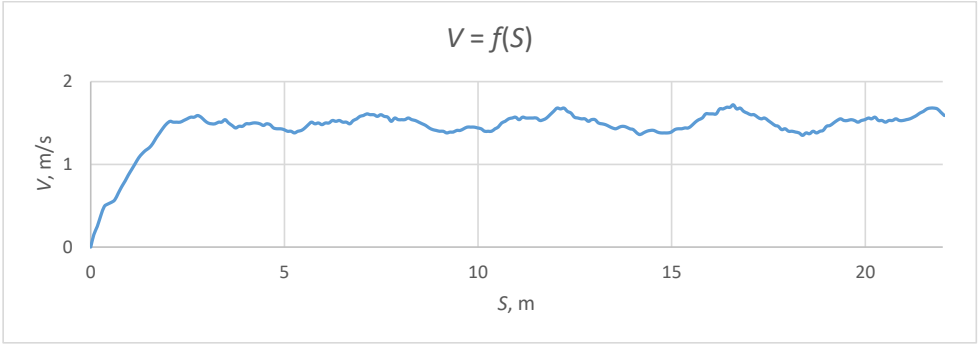

Fig. 4.20. The dynamics of the train speed when applying the developed algorithm.

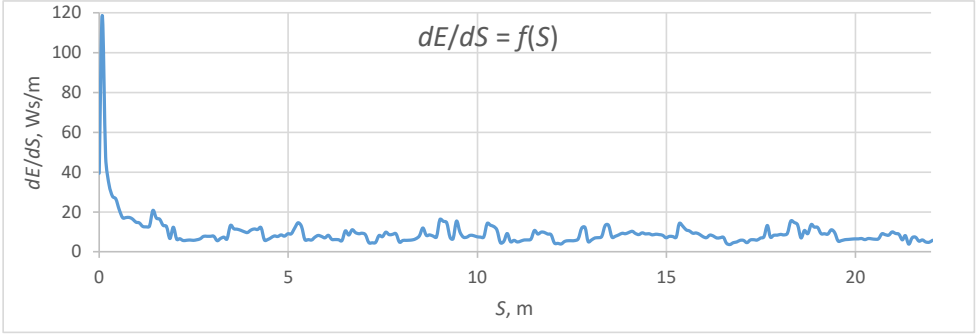

Fig. 4.21. The dynamics of dE/dS for the train electric drive when applying the developed algorithm.

From the graph, it can be seen that the control signal quickly reaches the desired value and changes according to the load characteristics. The speed V varies depending on the changes in the control signal and the load characteristics. Energy consumption E increases with the distance traveled [49]. Table 3 shows the energy consumption values for a constant control signal C with the lowest energy consumption (in the range from 60 to 255), the algorithm for finding the minimum with the best value based on the results of previous measurements, and the developed self-learning algorithm for optimal energy consumption with a neural network.

8 series of experiments were carried out for each algorithm and in all experiments the train traveled a distance of 115 m, which is approximately 10 laps of the experimental railway.

Table 3

Energy Consumption when Operating Different Search Algorithms and a Constant Control Signal at Different Values of *dS*, Average Speed and Instantaneous Speed at Voltage $U = 24$ V

	$U = 24$ V					
	C_{const}	***MSA***	**Developed self-learning algorithm**			
	-	**-**	**V_{avg}**		**V_{mom}**	
dS	-	-	**0.3**	**1**	**0.08**	**0.3**
E_{max}	1326.3	1799.6	1276.0	1267.3	1193.95	1335.1
E_{min}	1198.9	1475.41	1168.4	1208.3	1028.05	1154.6
E_{avg}	1237.1	1685.1	1219.4	1249.3	**1077.14**	1206.3

Designations in the table:

developed self-learning algorithm – developed self-learning optimal algorithm with a neural network;
MSA – minimum search algorithm;
dS – the step of energy measurement and control signal C change, m;
V_{mom} – instantaneous value of measured speed, m/s;
V_{avg} – average speed over distance *dS*, m/s;
E_{min} – the minimum amount of energy consumed to travel 115 m in a series of 8 experiments, Ws;
E_{max} – the maximum amount of energy consumed to travel 115 m in a series of 8 experiments, Ws;
E_{avg} – average energy consumed to travel 115 m in a series of 8 experiments, Ws;
C_{const} – constant control signal set to 255, experimentally proved as the best if keeping it unchanged.

From Table 3, it can be seen that the developed algorithm for optimal energy consumption with automatic generation of the training set for the neural network shows the best result. With a parameter measurement step of 0.08 m and using instantaneous velocity, it consumed 1077.14 Ws. The worst performing algorithm was the minimum search algorithm, which consumed 1685.1 Ws. The usage of the developed method allowed for a reduction in energy consumption of the electric train model by 159.96 Ws or 12.93 %, compared to a constant control signal of $C = 255$.

Conclusions

1. A control structure for the UV and a self-learning optimization controller with a neural network have been developed for optimal energy consumption of electric unmanned vehicles.
2. A mathematical model has been developed to calculate the movement of the UV, allowing calculating optimal control parameters under uncertain conditions and simulating the movement of unmanned vehicles in three-dimensional space.
3. A mathematical model of a neural network has been developed for optimal energy-efficient control of UV, enabling optimal control of the electric drive system.
4. A new algorithm for optimal energy-efficient control of the UV has been developed, consisting of a minimum search algorithm, an algorithm for automatic creation of a training set for the neural network and a neural network training algorithm, which includes procedures for adaptation, filtering, evaluation, and weight adjustment.
5. The considered minimum search algorithms allow finding the minimum energy consumption of the UV required to travel a given path.
6. The adaptive filtering algorithm can be used for training the neural network and unconditional weight optimization for optimal control of the UV.
7. Experimental devices for testing have been developed and manufactured, including a test stand, a quadcopter, and a model of a railway with an electric train.
8. The characteristics of the electric drives of the UV quadcopter and the electric train model have been investigated.
9. Comparing the effects of different parameter configurations on the nature of the target function, it can be concluded that the nature of the function remains unchanged. The optimal energy consumption point shifts in the direction of increasing control signal when the UV mass increases. The UV area and aerodynamics do not affect the optimal value of the control signal sought but increase energy consumption. This allows concluding that the developed target function and algorithm work equally well, adapting to different UV configurations: different motors and mass.
10. A computer model has been created to demonstrate that the energy consumption function for vertical ascent of the quadcopter has a unimodal nature for different motors, which facilitates optimization for specific maneuver types. Minimum search algorithms defined in the study are capable of finding the optimal value of the target function with a deviation of 0.6–1.6 % from the optimal value for a lower mass and 6.37–11.23 % for a higher mass on a straight section with a constant load. However, considering the unimodal nature of the target function in the case of one-dimensional functions, i.e., when it is necessary to find only one optimal control signal value, it is recommended to use deterministic search algorithms, as they provide the most stable optimization results, as demonstrated by the modeling results. Among the deterministic algorithms, algorithm 2 – the algorithm with halving method can be considered the most suitable among the compared algorithms. This algorithm allows finding the optimal control point in less time and with the smallest deviation.
11. Based on the experiments with the train, it is evident that there is no single optimal signal, and the search algorithm fails to find the optimal signals. With uniform search algorithm train consumes 1685 Ws, which is 36.2 % more than using a single constant C signal of 255 throughout the path, covering a distance of 115.59 m. Therefore, the uniform search algorithm for finding the minimum energy consumption consumes more energy and cannot find the optimal control signal under such load characteristic changes.
12. Data analysis for creating a training set has shown that the load characteristic can be assessed at each point of the path independently of the control signal and velocity of movement.
13. The developed algorithm for automatic creation of a training set for the neural network has demonstrated the ability to form a training set under conditions of changing load and has found

optimal control signal values for 35 road sections with different load characteristics, covering a distance of 62.2 m.

14. The results of experiments on selecting optimal parameters for the neural network show that the larger the training dataset with optimal neural network parameters, the more accurate the computed results are. The best accuracy is achieved with a deviation of 0.7503 and is produced by a neural network with 12 neurons. Under optimal parameters, there is an exponential relationship between the accuracy of computations and the number of iterations. The accuracy of computations also depends on time. To achieve the smallest deviation from the result of 0.752251, it requires 4017 ms.

15. The experimental results on the electric train model prove that the developed self-learning algorithm with neural network allows to increase energy-efficiency reducing electric energy consumption by 12.93 % in electric unmanned vehicles. With an algorithm's parameter of measurement step 0.08 m and utilizing instantaneous velocity values, the unmanned vehicle consumed 1077.14 Ws to cover a distance of 115 m. In comparison, when moving with a constant control signal $C = 255$, the energy consumption was measured at 1237.1 Ws.

The following development prospects can be highlighted:

- Research on constraint generation – defining or verifying minimum and maximum control signals.
- Checking the combination of optimized control signal proportions for compatibility with the performed maneuver or route.
- Improve the system and algorithm ensuring safe, reliable, and comfortable (in the case of passenger transportation) control criteria.
- Adaptation of control signals, their decoding and encoding for compatibility with different interfaces and control signal transmission protocols.

References

[1] Hnatov A. et al., "Development of a unified energy-efficient system for urban transport," 2020 6th IEEE International Energy Conference (ENERGYCon), 2020, pp. 248–253, doi: 10.1109/ENERGYCon48941.2020.9236606

[2] Rico J. et al., "Real time energy efficiency optimization in connected electrical vehicles," 2017 12th International Conference on Ecological Vehicles and Renewable Energies (EVER), 2017, pp. 1–6, doi: 10.1109/EVER.2017.7935950

[3] Zhang S., Luo Y., Wang J., Wang X., and Li K., "Predictive Energy Management Strategy for Fully Electric Vehicles Based on Preceding Vehicle Movement," in IEEE Transactions on Intelligent Transportation Systems, vol. 18, no. 11, pp. 3049–3060, Nov. 2017, doi: 10.1109/TITS.2017.2672542

[4] Abousleiman R., and Rawashdeh O., "Energy-efficient routing for electric vehicles using metaheuristic optimization frameworks," MELECON 2014 – 2014 17th IEEE Mediterranean Electrotechnical Conference, 2014, pp. 298–304, doi: 10.1109/MELCON.2014.6820550

[5] Abdelgadir A. A., and Alsawalhi J. Y., "Energy management optimization for an extended range electric vehicle," 2017 7th International Conference on Modeling, Simulation, and Applied Optimization (ICMSAO), 2017, pp. 1–5, doi: 10.1109/ICMSAO.2017.7934911

[6] Rohkämper S., Hellwig M., and Ritschel W., "Energy optimization for electric vehicles using dynamic programming," 2017 International Conference on Research and Education in Mechatronics (REM), 2017, pp. 1–5, doi: 10.1109/REM.2017.8075252

[7] Bertram C., and Herzog H., "Optimization method for drive train topology design and control of electric vehicles," 2013 World Electric Vehicle Symposium and Exhibition (EVS27), 2013, pp. 1–8, doi: 10.1109/EVS.2013.6914933

[8] Bertram C., Buecherl D., Thanheiser A., and Herzog H., "Multi-objective optimization of a parallel hybrid electric drive train," 2011 IEEE Vehicle Power and Propulsion Conference, 2011, pp. 1–5, doi: 10.1109/VPPC.2011.6043154

[9] Qu L., Zhuang W., and Chen N., "Instantaneous Velocity Optimization Strategy of Electric Vehicle Considering Varying Road Slopes," 2019 Chinese Control and Decision Conference (CCDC), 2019, pp. 5483–5488, doi: 10.1109/CCDC.2019.8832756

[10] Allaboina V., Ramana R. " Regenerative braking system: The regenerative braking system used in the vehicles for the purpose of saving a part of the energy lost during bracking, " LAP LAMBERT Academic Publishing, September 2, 2019, 64 p.

[11] Li B., Yu Z., Jin C., and Zhu Z., "Torque Allocation Algorithm of Distributed Driving Electric Vehicle Based on Energy Consumption Optimization," 2015 7th International Conference on Intelligent Human-Machine Systems and Cybernetics, 2015, pp. 319–323, doi: 10.1109/IHMSC.2015.46

[12] Guo L., Lin X., Ge P., Qiao Y., Xu L., and Li J., "Torque distribution for electric vehicle with four in-wheel motors by considering energy optimization and dynamics performance," 2017 IEEE Intelligent Vehicles Symposium (IV), 2017, pp. 1619–1624, doi: 10.1109/IVS.2017.7995941

[13] Hasan M. M., Baghdadi El M., and Hegazy O., "Energy Management Strategy in Electric Buses for Public Transport using ECO-driving," 2020 Fifteenth International Conference on Ecological Vehicles and Renewable Energies (EVER), 2020, pp. 1–8, doi: 10.1109/EVER48776.2020.9243130

[14] Fan A., Yin Q., Yan X., and Sun X., "Study of energy efficient navigation method for inland ship: A cruise ship case," 2015 International Conference on Transportation Information and Safety (ICTIS), 2015, pp. 437–441, doi: 10.1109/ICTIS.2015.7232079

[15] Zhong W., Xu H., and Zhang W., "Energy-efficient train reference speed profile optimization using control parameterization method," 2016 35th Chinese Control Conference (CCC), Chengdu, China, 2016, pp. 10128–10133, doi: 10.1109/ChiCC.2016.7554959

[16] Wen Y., Chenkun Y., and Zhongsheng H., "A novel energy efficient operation strategy for a train based on model-free adaptive predictive control," Proceedings of the 31st Chinese Control Conference, Hefei, China, 2012, pp. 7286–7291.

[17] He Z., Yang Z., and Lv J., "An energy-efficient operation strategy for high-speed trains," 2018 Chinese Control And Decision Conference (CCDC), Shenyang, China, 2018, pp. 3771–3776, doi: 10.1109/CCDC.2018.8407778

[18] Xiao Z., Chen M., Chai Y., Liu C., and Wang Q., "Energy-Efficient Operation of High-speed Trains Based on a Multiple Phases Model," 2018 37th Chinese Control Conference (CCC), Wuhan, China, 2018, pp. 7793–7798, doi: 10.23919/ChiCC.2018.8483849

[19] Chen Y., Feng L., Zhan J., and Shang F., "Online Energy-efficient Control of Urban Rail Train Operation Based on Switching Time Optimization," 2020 Chinese Automation Congress (CAC), Shanghai, China, 2020, pp. 6094–6099, doi: 10.1109/CAC51589.2020.9327596

[20] Zhong W., Xu H., and Zhang W., "Energy-efficient train reference speed profile optimization using control parameterization method," 2016 35th Chinese Control Conference (CCC), Chengdu, China, 2016, pp. 10128–10133, doi: 10.1109/ChiCC.2016.7554959
[21] Chao G., Xinpei W., Kun H., and Qingyuan W., "Optimal energy-efficient control of high-speed train with speed limit constraints," The 27th Chinese Control and Decision Conference (2015 CCDC), Qingdao, China, 2015, pp. 3076–3081, doi: 10.1109/CCDC.2015.7162449
[22] Gorobecs M., Ģenētisko algoritmu izpēte elektriskā transporta optimālai vadībai, Promocijas darbs, Rīga, Latvija, 2008.
[23] Ribickis L., Valeinis J., "Elektriskā piedziņa mahatronikas sistēmās," RTU tipogrāfijā, Rīga, 2008.
[24] Klaus, "How fast can a quadcopter fly?", [Viewed on March 2, 2022] Available: https://klsin.bpmsg.com/how-fast-can-a-quadcopter-fly/
[25] Pyrhonen J., Hrabovcova V., Semken R. S, "Electrical Machine Drives Control: An Introduction," Wiley, November 14, 2016, 526 p.
[26] Haykin S., "Neural Networks. A Comprehensive Foundation," Second Edition, Prenctice Hall, 2006
[27] Onwubolu G. C., "Mechatronics Principles and Applications," Elsevier Butterworth Heinemann, 2005. 642 p.
[28] Valeinis J., "Elektriskās piedziņas vadība," Rīga, Rīgas Tehniskā universitāte, 1982. 95 lpp.
[29] Valeinis J., "Ievads elektriskās piedziņas vadības sistēmās," Rīga: RTU, 2007. 163 lpp
[30] Blumbergs E., "Elektriskās piedziņas vadība," Rīga, Rīgas Tehniskā universitāte, 1983. 106 lpp.
[31] Borisovs A., "Mākslīgā intelekta metodes," Rīgas Tehniskā universitāte. Automātikas un skaitļošanas tehnikas fakultāte, Rīga: RTU, 1993. 75 lpp.
[32] Borisov, A. N., "Genetic algorithms, genetic programming, genetic machine learning," lecture slides. Transport and Telecommunications Inst. Riga: TTI, 2004. 251 p.
[33] Greivulis J., Raņķis I., "Iekārtu vadības elektroniskie elementi un mezgli," Rīga: Avots, 2005. 288 lpp.
[34] Grundspeņķis J., "Ievads intelektuālās sistēmās," Lekciju konspekts, RTU, 1993. 158 lpp.
[35] Lagzdiņš Ģ., "Pamatkurss elektrotehnikā," Rīga: Jumava, 2004. 218 lpp.
[36] Levine W., "The Control Handbook," CRC press, 1996.
[37] Luger G. F., "Artificial Intelligence. Structures and Strategies for Complex Problem Solving," Williams, 2003.
[38] Merkurjevs J., "Imitācijas modelēšanas tehnoloģijas," Lekciju konspekts, 2003.
[39] Merkurjevs J., "Sistēmu imitācijas modelēšanas tehnoloģija," Rīga, RTU, 2008. 120 lpp.
[40] Palm W. J., "Modeling, Analysis, and Control of Dynamic Systems," 2nd Edition, Wiley, 1999.
[41] Rankis I., Gorobetz M., Levchenkov A., "Optimal Electric Vehicle Speed Control by Intelligent Devices," Rīgas Tehniskās universitātes raksti. Enerģētika un Elektrotehnika. Sērija 4, sējums 16. 2006. 127–137. lpp.
[42] Raņķis I., Zhiravetska A., "Electronics," Riga, RTU publishing House, 2005. 106 p.
[43] Raņķis I., Ievads specialitāte "Elektrotehnoloģiju datorvadība," Rīga, RTU, 2003. 41 lpp.
[44] A. Korneyev, M. Gorobetz. Neural Network Based UAV Optimal Control Algorithm for Energy Efficiency Maximization, 2020 IEEE 61st International Scientific Conference on Power and Electrical Engineering of Riga Technical University (RTUCON 2020), Latvia, Riga, 5–7 November 2020. Piscataway: IEEE, 2020, pp. 1–5.
[45] A. Korneyev, M. Gorobetz, A. Levchenkov. Unified Energy Efficient Control Algorithm for Electric Unmanned Aerial Vehicles with Different Traction Drives and Configurations. 2018 IEEE 59th International Scientific Conference on Power and Electrical Engineering of Riga Technical University (RTUCON 2018), Latvia, Riga, 12–14 November 2018. Piscataway: IEEE, 2018, pp. 537–542.
[46] A. Korneyev, M. Gorobetz, I. Alps, L. Ribickis. Adaptive Traction Drive Control Algorithm for Electrical Energy Consumption Minimisation of Autonomous Unmanned Aerial Vehicle. Electrical, Control and Communication Engineering, 2019, Vol. 15, No. 2, pp. 62–70.
[47] M. Gorobetz, A. Potapovs, A. Korneyev. Analysis and Modelling of UAV Electrical Traction Drive based on Empirical Data for Energy Efficiency Tasks. 2019 IEEE 60th International Scientific Conference on Power and Electrical Engineering of Riga Technical University (RTUCON 2019), Latvia, Riga, 7–9 October 2019. Piscataway: IEEE, 2019, pp. 399–403.
[48] M. Gorobetz, A. Potapovs, A. Korneyev, I. Alps. Device and Algorithm for Vehicle Detection and Traffic Intensity Analysis. Electrical, Control and Communication Engineering, 2021, Vol. 17, No. 1, pp. 83–92.
[49] M. Gorobetz, L. Ribickis, A. Beinarovica, A. Kornejevs. Immune Neural Network Machine Learning of Autonomous Drones for Energy Efficiency and Collision Prevention. Drones – Various Applications, Rijeka, Published: September 18, 2023, doi:10.5772/intechopen.1002533
[50] Карпенко А. П. Методы оптимизации (базовый курс), [Viewed on March 2, 2022], Available: http://bigor.bmstu.ru/?cnt/?doc=MO/base.cou
[51] Новиков Ф. А., "Дискретная математика для программистов", - СПб: "Питер", 2003. 304 с.
[52] Рутковская Д., Пилиньский М., Рутковский Л., "Нейронные сети, генетические алгоритмы и нечеткие системы", Телеком, 2004

Aleksandrs Korņejevs was born in 1983 in Riga. He obtained a Bachelor's degree (2016) and a Master's degree (2018) in Electrical Science from Riga Technical University (RTU). He was a board member at the company "Solar AK". Since 2019, he has been working at RTU, holding the positions of scientific assistant, senior laboratory assistant in scientific work, lecturer, and study process expert. Currently, he is a research assistant at the Institute of Industrial Electronics and Electrical Engineering (IEEI) of Faculty of Electrical and Environmental Engineering. In 2018 he was included in the RTU Golden Fund. His research interests are related to electroacoustics, radio electronics, control systems of unmanned vehicles and artificial neural networks.